Volume 21
Number 6
June 1982

Inorganic Chemistry

Contribution from the Department of Chemistry,
University of Rochester, Rochester, New York 14627

Rhodium A-Frame Complexes with Small-Molecule Bridgeheads. Synthesis and Structure of $[Rh_2(\mu\text{-}H)(\mu\text{-}CO)(CO)_2(PPh_2CH_2PPh_2)_2](p\text{-}CH_3C_6H_4SO_3)\cdot 2THF$ and Catalytic Properties

CLIFFORD P. KUBIAK, CARRIE WOODCOCK, and RICHARD EISENBERG*

Received July 29, 1981

The reaction of $[Rh_2Cl_2(CO)_2(dpm)_2]$ with $NaBH_4$ in EtOH leads to $[Rh_2(CO)_2(dpm)_2]$. Subsequent reactions with H^+, CO, acetylenes, and CO_2 lead to new complexes having the A-frame structure with the addendum molecule in the bridging position. Solutions of $[Rh_2(CO)_2(dpm)_2]$ under H_2 are active in the hydrogenation of acetylene. Sequential treatment of $[Rh_2(CO)_2(dpm)_2]$ with H^+ and CO gives $[Rh_2(\mu\text{-}H)(\mu\text{-}CO)(CO)_2(dpm)_2]^+$, and a single-crystal X-ray structure determination of its *p*-toluenesulfonate salt has been performed. The complex $[Rh_2(\mu\text{-}H)(\mu\text{-}CO)(CO)_2(dpm)_2](p\text{-}MeC_6H_4SO_3)\cdot 2THF$ crystallizes in the monoclinic space group $C2/m$ in a unit cell of dimensions $a = 24.391$ (11) Å, $b = 18.863$ (9) Å, $c = 14.440$ (6) Å, and $\beta = 107.81$ (2) Å with $Z = 4$. The structural study reveals the presence of both bridging hydride and bridging CO, a Rh–Rh separation of 2.732 (2) Å, and an average angle between the bridging hydride and the terminal CO ligands of 152 (3)°. The complex is also found to result from the decomposition of a related formate species $[Rh_2(\mu\text{-}O_2CH)(CO)_2(dpm)_2]^+$ in the presence of CO. In 1-propanol or bis(2-ethoxyethyl) ether solution, $[Rh_2(\mu\text{-}H)(\mu\text{-}CO)(CO)_2(dpm)_2]^+$ is a catalyst for the water-gas shift reaction $CO + H_2O \rightleftharpoons H_2 + CO_2$. At 90 °C under 1 atm of CO, a rate corresponding to 0.58 turnover per complex/h is observed. This rate is maintained for approximately 35 h after which it gradually decreases, completely ceasing in 70 h. The complex is also a catalyst for the hydrogenation and hydroformylation of olefins with $CO + H_2O$ as the source of hydrogen. The rate and duration of catalysis for these reactions are similar to those found for the water-gas shift reaction. Reactions relating to the product forming steps in these systems are discussed.

Introduction

The first binuclear complexes of the A-frame geometry, I,

I

were reported in 1977.[1,2] Since then, other complexes of this type have been described including several which bind small molecules, e.g., CO,[3-6] SO_2,[7-9] H_2,[6] on the endo side or pocket of the A-frame complex. One particularly fruitful approach to the synthesis of A-frame complexes has been the insertion of small molecules into the metal–metal bond of the bis(diphosphine)-bridged system $[M_2X_2(dpm)_2]$ (M = Pd, Pt; dpm = bis(diphenylphosphino)methane; X = Cl, Br), eq 1, as reported by Balch,[10-12] Puddephatt,[13-15] and others.[16-18] We

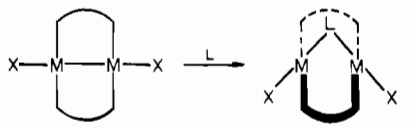

(1)

L = CO, CNR, SO_2, H^+, ^+N_2R, CH_2, RCCR

report herein the preparation of an analogous Rh(0) system, $[Rh_2(CO)_2(dpm)_2]$, and the addition of small molecules, L = CO, HCCR, CO_2, and H^+, to form rhodium A-frame complexes, eq 2.

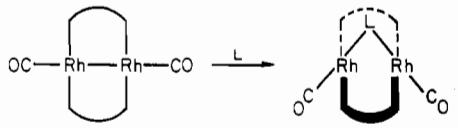

(2)

(1) Kubiak, C. P.; Eisenberg, R. *J. Am. Chem. Soc.* **1977**, *99*, 6129.
(2) Olmstead, M. M.; Hope, H.; Benner, L. S.; Balch, A. L. *J. Am. Chem. Soc.* **1977**, *99*, 5502.
(3) (a) Cowie, M.; Mague, J. T.; Sanger, A. R. *J. Am. Chem. Soc.* **1978**, *100*, 3628. (b) Cowie, M. *Inorg. Chem.* **1979**, *18*, 286.
(4) Cowie, M.; Dwight, S. K. *Inorg. Chem.* **1979**, *18*, 2700.
(5) Olmstead, M. M.; Lindsay, C. H.; Benner, L. S.; Balch, A. L. *J. Organomet. Chem.* **1979**, *179*, 289.
(6) Kubiak, C. P.; Woodcock, C.; Eisenberg, R. *Inorg. Chem.* **1980**, *19*, 2733.
(7) (a) Cowie, M.; Dwight, S. K.; Sanger, A. R. *Inorg. Chim. Acta* **1978**, *31*, L407. (b) Sanger, A. R. *Prepr.—Can. Symp. Catal. 6th* **1979**, *37*.
(8) (a) Mague, J. T.; Sanger, A. R. *Inorg. Chem.* **1979**, *18*, 2060. (b) Mague, J. T.; DeVries, S. H. *Ibid.* **1980**, *19*, 3743.
(9) Kubiak, C. P.; Eisenberg, R. *Inorg. Chem.* **1980**, *19*, 2726.
(10) Benner, L. S.; Balch, A. L. *J. Am. Chem. Soc.* **1978**, *100*, 6099.
(11) Balch, A. L.; Benner, L. S.; Olmstead, M. M. *Inorg. Chem.* **1979**, *18*, 2996.
(12) (a) Balch, A. L.; Lee, C. L.; Lindsay, C. H.; Olmsead, M. M. *J. Organomet. Chem.* **1979**, *177*, C22. (b) Cowie, M.; Southern, T. G. *Ibid.* **1980**, *193*, C46.
(13) Brown, M. P.; Puddephatt, R. J.; Rashidi, M.; Seddon, K. R. *Inorg. Chim. Acta* **1977**, *23*, L27.
(14) Brown, M. P.; Puddephatt, R. J.; Rashidi, M.; Manojlovic-Muir, L.; Muir, K. W.; Solomon, T.; Seddon, K. R. *Inorg. Chim. Acta* **1977**, *23*, L33.
(15) Brown, M. P.; Fisher, J. R.; Puddephatt, R. J.; Seddon, K. R. *Inorg. Chem.* **1979**, *18*, 2808.
(16) Colton, R.; McCormick, M. J.; Pannan, C. D. *Aust. J. Chem.* **1978**, *31*, 1425.
(17) Rattray, A. D.; Sutton, D. *Inorg. Chim. Acta* **1978**, *28*, L85.
(18) Colton, R.; McCormick, M. J.; Pannan, C. D. *J. Chem. Soc., Chem. Commun.* **1977**, 823.

0020-1669/82/1321-2119$01.25/0

Sequential treatment of $[Rh_2(CO)_2(dpm)_2]$ with CO and H^+, in either order, produces the unusual μ-hydride, μ-carbonyl A-frame derivative $[Rh_2(\mu\text{-}H)(\mu\text{-}CO)(CO)_2(dpm)_2]^+$. Full details of an X-ray crystallographic study of the *p*-toluenesulfonate salt of this complex are now presented.

The μ-hydride, μ-carbonyl complex is an active catalyst under relatively mild conditions for both the water-gas shift reaction (ca. 90 °C and 1 atm of CO), and the hydroformylation/hydrogenation reactions with H_2O + CO as the source of hydrogen (ca. 90 °C, 0.5 atm of CO and 0.5 atm of ethylene). A partial report of this work has been previously communicated.[19] We now describe initial studies of the catalytic systems and specific reactions involving $[Rh_2(\mu\text{-}H)(\mu\text{-}CO)(CO)_2(dpm)_2]^+$ which relate to the product forming steps of the catalyses.

Experimental Section

Materials. Rhodium trichloride hydrate (Johnson Matthey), phosphines (Strem), hexafluorophosphoric acid–diethyl ether, phenylacetylene, *p*-toluenesulfonic acid (Eastman), sodium formate, and sodium acetate (Mallinckrodt), and gases CO, H_2, acetylene, ethylene (Matheson CP), and CO_2 (Matheson Bone Dry) were used as purchased unless otherwise stated.

Preparation and Characterization of Complexes. All syntheses were routinely performed under an atmosphere of dry nitrogen with modified Schlenk techniques. Due to the extreme sensitivity of many of the complexes to air and moisture, most physical manipulations involving them, including the preparation of IR and NMR samples, were performed in a drybox (Vacuum Atmospheres, Inc.). $[Rh_2Cl_2(CO)_2(dpm)_2]$[20] (dpm = bis(diphenylphosphino)methane) and $RhH(CO)(PPh_3)_3$[21] were prepared by published procedures. Elemental analyses were performed by Galbraith Laboratories, Knoxville, TN. ^1H and ^{31}P NMR spectra were recorded on a JEOL JNM-PS-100 Fourier transform spectrometer with heteronuclear decoupler.[22] Infrared spectra were recorded on a Perkin-Elmer 467 grating spectrometer calibrated with polystyrene film.[22] Samples were either solutions prepared in a drybox, KBr pellets, or Nujol mulls on NaCl plates.

$[Rh_2(CO)_2(PPh_2CH_2PPh_2)_2]$. Sodium borohydride, ca. 0.05 g, is dissolved in 30 mL of dry EtOH under N_2, and $[Rh_2Cl_2(CO)_2(dpm)_2]$, 0.2 g, is added to the solution. A purple precipitate is formed over a period of 1 h and then collected under N_2. The complex is washed twice with 50-mL portions of dry EtOH and then with Et_2O and dried in vacuo. Recrystallization from THF–Et_2O or toluene–Et_2O affords air-sensitive, purple crystals. Anal. Calcd for $C_{52}H_{44}P_4O_2Rh_2$: C, 60.60; H, 4.30; P, 12.02. Found: C, 60.25; H, 4.69; P, 11.57. IR: ν(CO) = 1915 cm^{-1} (Nujol). Repeating the procedure above, but with $NaBD_4$, leads to no change in the IR spectrum. ^1H NMR (acetone-d_6, ppm relative to internal Me_4Si, intensity): δ 7.54 (C_6H_5, m, 40), 4.32 (CH_2, m, br, 4). The ^1H NMR spectrum upfield of Me_4Si to −30.0 ppm is silent. $^{31}P\{^1H\}$ NMR (ppm relative to internal $(CH_3O)_3PO$): δ 29.51 (m).

$[Rh_2(\mu\text{-}CO)(CO)(PPh_2CH_2PPh_2)_2(Sol)]$ (Sol = CH_2Cl_2, PPh_3). $RhH(CO)(PPh_3)_3$, 0.2 g, and dpm, 0.085 g, are dissolved together in 10 mL of CH_2Cl_2. The reaction is accompanied by a change in color of the solution to dark brown and evolution of H_2 gas which is monitored by GC. After 1 h, the amount of H_2 produced corresponds to ca. 1:2 H_2:$RhH(CO)(PPh_3)_3$. IR (CH_2Cl_2 solution): ν(CO) = 1936 vs, 1800 s, br cm^{-1}. A brown solid can be isolated after addition of 10 mL of EtOH, removal of CH_2Cl_2 under vacuum, and storage of the solution at −10 °C for 4 h. The complex so obtained contains 1 molecule of CH_2Cl_2/molecule of $[Rh_2(CO)_2(dpm)_2]$. Anal. Calcd for $C_{53}H_{46}P_4O_2Cl_2Rh_2$: C, 57.06; H, 4.16; P, 11.11. Found: C, 56.94; H, 4.32; P, 11.03. IR (Nujol): ν(CO) = 1915 vs, 1800 s, br. ^1H NMR: δ 6.20–7.60 (C_6H_5, m, 40), 5.32 (CH_2Cl_2, s, 2), 4.25 (CH_2, m, 2), 4.58 (m, 2). The $^{31}P\{^1H\}$ NMR of a sample prepared by repeating the reaction above in benzene-d_6 shows a broadened doublet at δ 39.35 ($J_{P\text{-}Rh} \approx 156$ Hz) and two complex multiplets centered at δ 19.35 and δ 9.40 in addition to free triphenylphosphine δ −8.47 (relative to $(CH_3O)_3PO$).

Additions of Small Molecules to $[Rh_2(CO)_2(PPh_2CH_2PPh_2)_2]$ or $[Rh_2(\mu\text{-}CO)(CO)(PPh_2CH_2PPh_2)_2(Sol)]$. Addition of CO. Preparation of $[Rh_2(\mu\text{-}CO)(CO)_2(PPh_2CH_2PPh_2)_2]$. The complex can be prepared by any of the following three methods.

Method A. $[Rh_2(CO)_2(dpm)_2]$, which has been prepared as described above by borohydride reduction of $[Rh_2Cl_2(CO)_2(dpm)_2]$, is dissolved in toluene, CH_2Cl_2, or THF. The solution is placed under an atmosphere of CO and immediately changes in color to red-orange. Dark orange microcrystals are obtained by addition of EtOH or Et_2O and cooling to −10 °C. Anal. Calcd for $C_{53}H_{44}P_4O_3Rh_2$: C, 60.13; H, 4.53; P, 11.70. Found: C, 59.97; H, 4.18; P, 11.10. IR: ν(CO) = 1940 s,sh, 1920 vs, 1835 cm^{-1} (Nujol). ^1H NMR (acetone-d_6): for C_6H_5 δ 7.53 (16), 7.25 (8), and 7.20 (16); for CH_2, 4.46 (4). $^{31}P\{^1H\}$ NMR (ppm relative to internal $(CH_3O)_3PO$): 15.72 (dpm, symmetric multiplet with two principal lines separated by ~144 Hz).

Method B. A solution of $[Rh_2(\mu\text{-}CO)(CO)(dpm)_2(PPh_3)]$ is prepared as described above from $RhH(CO)(PPh_3)_3$ and dpm. Addition of CO and EtOH or Et_2O and cooling lead to the complex as orange microcrystals with IR and NMR data identical with those from samples prepared by method A.

Method C. $[Rh_2Cl_2(CO)_2(dpm)_2]$, 0.1 g, is partially dissolved in 30 mL of dry EtOH under CO. $NaBH_4$, ca. 0.05 g, is added, and after 30 min the complex is obtained as a dark orange precipitate. Recrystallization from CH_2Cl_2–EtOH affords a microcrystalline product with IR and NMR data identical with those from samples prepared by method A.

Addition of Acetylenes, RC_2H (R = Ph, H). Characterization of $[Rh_2(HCCR)(CO)_2(PPh_2CH_2PPh_2)_2]$ in Solution. $[Rh_2(HCCH)(CO)_2(dpm)_2]$. $[Rh_2(CO)_2(dpm)_2]$, 0.1 g, is dissolved in a minimal amount of benzene-d_6 to obtain a saturated solution. The solution is placed under 1 atm of acetylene gas. After 2 h, the solution color is deep emerald green. IR (benzene solution): ν(CO) = 1946 s,sh, 1938 vs cm^{-1}. ^1H NMR (relative to internal Me_4Si, with intensity): δ 7.5–8.3 (C_6H_5. m, 40), 3.35 (CH_2, m, 2), 2.91 (CH_2, m, 2). The $^{31}P\{^1H\}$ NMR spectrum shows a symmetric multiplet centered at δ 17.66 with two principal lines separated by 133.0 Hz.

$[Rh_2(HCCPh)(CO)_2(dpm)_2]$. The phenylacetylene complex is prepared as above, but with 10 μL of PhCCH. Benzene solutions of the complex are intense blue-green. IR (benzene solution): ν(CO) = 1958 vs, 1930 s, sh cm^{-1}. ^1H NMR δ 7.5–8.3 (C_6H_5, m, 45), 3.77 (CH_2, m, 2), 2.89 (CH_2, m 2). The $^{31}P\{^1H\}$ NMR shows a complicated asymmetric multiplet extending from δ 20.87 to δ 16.26.

Addition of CO_2. Preparation of $[Rh_2(CO_2)(CO)_2(PPh_2CH_2PPh_2)_2]$. $[Rh_2(CO)_2(dpm)_2]$, 0.1 g, is dissolved in 10 mL of THF, which has been freshly distilled over sodium. The solution is cooled to −78 °C and then placed under 1 atm of CO_2, which was passed through a drying tower containing "drierite". The solution is then stored at −10 °C for 6 h to obtain a yellow precipitate. Anal. Calcd for $C_{53}H_{44}P_4O_4Rh_2$: C, 59.24; H, 4.13; P, 11.53. Found: C, 58.96; H, 4.46; P, 11.11. IR: ν(CO) = 1954 s, 1941 vs; $\nu(CO_2)$ = 1645 m, 1590 s cm^{-1} (Nujol). Characterization by NMR has been precluded by decomposition of the complex with loss of CO_2 when dissolved in most solvents.

Protonation of $[Rh_2(CO)_2(PPh_2CH_2PPh_2)_2]$. Characterization of $[Rh_2(H)(CO)_2(PPh_2CH_2PPh_2)_2]^+A^-$ (A^- = *p*-$CH_3C_6H_4SO_3^-$, PF_6^-). $[Rh_2(CO)_2(dpm)_2]$, 0.1 g, is dissolved in 10 mL of THF and 1 equiv of hexafluorophosphoric acid–diethyl ether, 0.02 g, or *p*-toluenesulfonic acid which has been dried previously under vacuum, 0.016 g, is added. The solution color immediately changes to dark green-brown. The amount of H_2 detected over the solution by GC corresponds to <5% yield. IR (THF solution): 1974 s, sh, 1951 vs cm^{-1}. The ^1H NMR spectrum was recorded for a sample prepared with *p*-toluenesulfonic acid in CD_2Cl_2: δ 8.10–7.37 (C_6H_5, C_6H_4, m, 44), 3.96 (CH_2, m, 2), 4.20 (CH_2, m, 2), 2.35 (CH_3, s, 3), −10.10 (H, br, 1).

Preparation of μ-Carboxylates, $[Rh_2(\mu\text{-}O_2CR)(CO)_2(PPh_2CH_2PPh_2)_2]^+A^-$ (R = H, CH_3; A^- = BF_4^-, PF_6^-). $[Rh_2Cl_2(CO)_2(dpm)_2]$, 0.1 g, is partially dissolved in 30 mL of MeOH, followed by the addition of 1 equiv of silver nitrate. The solution is heated to reflux, which results in a pale yellow solution and silver chloride precipitate. Addition of ca. 0.05 g of sodium formate to the solution followed by heating at 60 °C for 15 min leads to a bright red solution. The complex is precipitated by adding $NaBF_4$ or $NaPF_6$

(19) Kubiak, C. P.; Eisenberg, R. *J. Am. Chem. Soc.* **1980**, *102*, 3637.
(20) (a) Mague, J. T. *Inorg. Chem.* **1969**, *8*, 1975. (b) Mague, J. T.; Mitchener, J. P. *Ibid.* **1969**, *8*, 119.
(21) Ahmad, N.; Robinson, S. D.; Uttley, M. F. *J. Chem. Soc., Dalton Trans.* **1972**, 843.
(22) For NMR data: s = singlet, d = doublet, t = triplet, quar = quartet, quin = quintet, m = multiplet; For IR data: vs = very strong, s = strong, m = medium, w = weak, sh = shoulder.

and recrystallized from CH_2Cl_2–MeOH. The acetate complex is prepared in a similar way. Both the formate and acetate complexes are obtained as red crystals.

$[Rh_2(\mu\text{-}O_2CH)(CO)_2(dpm)_2]^+PF_6^-$. Anal. Calcd for $C_{53}H_{45}P_5O_4F_6Rh_2$: C, 52.15; H, 3.72; P, 12.69. Found: C, 51.96; H, 3.79; P, 12.51. IR: ν(CO) = 1946 vs, 1968 vs; $\nu(HCO_2)$ = 1548 m cm^{-1} (Nujol).

$[Rh_2(\mu\text{-}O_2CCH_3)(CO)_2(dpm)_2]^+BF_4^-$. Anal. Calcd for $C_{54}H_{47}P_4O_4BF_4Rh_2$: C, 55.13; H, 4.03; P, 10.53. Found: C, 54.85; H, 4.29; P, 10.40. IR: ν(CO) = 1951 vs, 1974 vs; $\nu(CH_3CO_2)$ = 1520 m cm^{-1} (Nujol).

Protonation of $[Rh_2(\mu\text{-}CO)(CO)_2(PPh_2CH_2PPh_2)_2]$. Preparation of $[Rh_2(\mu\text{-}H)(\mu\text{-}CO)(CO)_2(PPh_2CH_2PPh_2)_2]^+A^-\cdot Sol$ ($A^- = PF_6^-$, Sol = C_7H_8 or CH_2Cl_2; $A^- = p\text{-}CH_3C_6H_4SO_3^-$, Sol = 2THF). $[Rh_2(\mu\text{-}CO)(CO)_2(dpm)_2]$, 0.1 g, is dissolved in CH_2Cl_2 or toluene. $Et_2OH^+PF_6^-$, 0.02 g, is added, leading to an immediate change in color of the solution to purple. Cooling the toluene solution affords the purple toluene solvated PF_6^- salt. Anal. Calcd for $C_{60}H_{53}P_5O_3F_6Rh_2$: C, 55.57; H, 4.12; P, 11.94. Found: C, 54.60; H, 4.05; P, 11.72. The purple dichloromethane-solvated PF_6^- salt is obtained by adding Et_2O to dichloromethane solutions of the complex and cooling to −10 °C for 12 h. Anal. Calcd for $C_{54}H_{47}P_4O_3F_6Cl_2Rh_2$: C, 50.30; H, 3.67; P, 12.01. Found: C, 50.70; H, 3.87; P, 12.12. IR: ν(CO) = 1972 s, 1957 vs, 1870 s cm^{-1} (Nujol). ^1H NMR (acetone-d_6): δ 7.69 (C_6H_5, 16), 7.45 (C_6H_5, 8), 7.37 (C_6H_5, 16), 4.19 (CH_2, 4), δ −9.65 (H, 1). $^{31}P\{^1H\}$ NMR: δ 27.24 (dpm, symmetric m).

Dark green crystals of the *p*-toluenesulfonic salt are obtained by dissolving 0.1 g of $[Rh_2(\mu\text{-}CO)(CO)_2(dpm)_2]$ and 0.02 g of *p*-toluenesulfonic acid in 5 mL of THF and cooling to −10 °C for 24 h. IR: ν(CO) = 1970 s, 1955 vs, 1860 s cm^{-1} (Nujol). Solutions of the complex so prepared exhibit IR and NMR data identical with those of the hexafluorophosphate salt, except for differences due to the different anions.

Reaction of $[Rh_2(H)(CO)_2(PPh_2CH_2PPh_2)_2]^+PF_6^-$ with CO. A CH_2Cl_2 solution of $[Rh_2(H)(CO)_2(dpm)_2]^+PF_6^-$ is prepared from $[Rh_2(CO)_2(dpm)_2]$ and $Et_2OH^+PF_6^-$. CO, 1 atm, is introduced, and the solution color immediately changes to purple. Addition of Et_2O followed by cooling to −10 °C leads to purple crystals of $[Rh_2(\mu\text{-}H)(\mu\text{-}CO)(CO)_2(dpm)_2]^+PF_6^-$, identified by spectroscopic comparison with authentic samples.

Reaction of $[Rh_2(H)(CO)_2(PPh_2CH_2PPh_2)_2]^+PF_6^-$ with CO_2. A THF solution of $[Rh_2(H)(CO)_2(dpm)_2]^+PF_6^-$ is prepared from $[Rh_2(CO)_2(dpm)_2]$ and $Et_2OH^+PF_6^-$. CO_2, 1 atm, is introduced and the solution is heated briefly, ca. 1–5 min. The solution is then cooled to −10 °C for 4 h to obtain a red solution. Addition of Et_2O leads to a red microcrystalline precipitate which is identified as $[Rh_2(\mu\text{-}O_2CH)(CO)_2(dpm)_2]^+PF_6^-$ by characteristic ν(CO) = 1946 vs, 1968 vs; $\nu(HCO_2)$ = 1548 cm^{-1} (Nujol).

Reaction of $[Rh_2(CO_2)(CO)_2(PPh_2CH_2PPh_2)_2]$ with CO. $[Rh_2(CO_2)(CO)_2(dpm)_2]$, 0.05 g, is dissolved in 3 mL of CH_2Cl_2 in a 10-mL flask. CO, 1 mL at 1 atm, is added with a gas syringe. The solution color changes to red-orange over a period of 10 min and CO_2 evolution is monitored by GC. After 10 min, the yield of CO_2 corresponds to ca. 90%. The species in solution is identified as $[Rh_2(\mu\text{-}CO)(CO)_2(dpm)_2]$ by characteristic ν(CO) (1950 s,sh, 1932 vs, 1835 s, br cm^{-1} (CH_2Cl_2)) and can be isolated by addition of Et_2O to give the orange solid (ν(CO) = 1940 s,sh, 1920 vs, 1835 s, br cm^{-1} (Nujol)).

Reaction of $[Rh_2(\mu\text{-}O_2CH)(CO)_2(PPh_2CH_2PPh_2)_2^+PF_6^-$ with CO. $[Rh_2(\mu\text{-}O_2CH)(CO)_2(dpm)_2]^+PF_6^-$, 0.05 g, is dissolved in 5 mL of CH_2Cl_2 in a 10-mL flask. CO, 1 mL at 1 atm, is added with a gas syringe. The solution color slowly darkens, and CO_2 evolution is monitored by GC. After 0.5 h, the solution is deep purple and the amount of CO_2 produced corresponds to ca. 90% yield. The species in solution is identified as $[Rh_2(\mu\text{-}H)(\mu\text{-}CO)(CO)_2(dpm)_2]^+PF_6^-$ by characteristic purple color and ν(CO) = 1980s, 1963 vs, 1870 s cm^{-1} (CH_2Cl_2).

Reaction of $[Rh_2(\mu\text{-}H)(\mu\text{-}CO)(CO)_2(dpm)_2]^+PF_6^-$ with HCl. $[Rh_2(\mu\text{-}H)(\mu\text{-}CO)(CO)_2(dpm)_2]^+PF_6^-$, 0.05 g, is dissolved in 5 mL of CH_2Cl_2, and 1 drop of 37% HCl is added. The solution color immediately changes to pale yellow. H_2 gas is detected over the solution by GC in >90% yield with the assumption of 1 mol of H_2/mol of complex. Smaller quantities of CO (ca. 20%) and CO_2 (10%) are also detected. The species in solution are identified as a mixture of $[Rh_2(\mu\text{-}Cl)(CO)_2(dpm)_2]^+$ and $[Rh_2(\mu\text{-}Cl)(\mu\text{-}CO)(CO)_2(dpm)_2]^+$ by comparison of the IR spectrum with authentic samples prepared by published procedures[3-5] (ν(CO) = 2008 s, sh, 1990 vs, 1873 m cm^{-1} (CH_2Cl_2)) and by isolation of $[Rh_2(\mu\text{-}Cl)(CO)_2(dpm)_2]^+PF_6^-$ after replacing the gas phase with N_2 and adding Et_2O. Anal. Calcd for $C_{53}H_{44}P_5ClO_3F_6Rh_2$: C, 51.38; H, 3.58; P, 12.50; Cl, 2.86. Found: C, 51.36; H, 3.76; P, 12.71; Cl, 3.13. IR: ν(CO) = 1997 s, 1978 vs cm^{-1} (Nujol).

Acetylene Hydrogenation, Water-Gas Shift Catalysis, and Hydroformylation Catalysis. Typically, solutions were prepared in 100- or 500-mL flasks, which were charged with a total of 400–600 torr of the reagent gasses and heated to 80 or 90 °C. During the reactions, gasses were sampled with a "Pressure-Lok" gas syringe (Precision Sampling Corp.) and analyzed by gas chromatography (Hewlett-Packard 5700A) using a 12-ft Porapak Q or 2-ft molecular sieve column at 43 °C, a thermal conductivity detector at 100 °C, and a helium carrier gas with a flow rate of 40 mL/min. GC peak heights for the product and reagent gasses were converted to partial pressures by using calibration plots previously obtained. Methane gas, ca. 60 torr, was used as an internal calibrant. The aldehyde and alcohol products obtained from the hydroformylation reactions were analyzed by GC (Hewlett Packard 5730A) using a 15 ft × $^1/_4$ in. 15% Carbowax on Chromosorb P column at 100 °C, a flame ionization detector, and a N_2 carrier gas flow rate of 60 mL/min. A JEOL JNM-PS-100 Fourier transform spectrometer was used to record the ^1H NMR spectra of the product aldehyde.

Acetylene Hydrogenation. $[Rh_2(CO)_2(dpm)_2]$, 0.05 g, is dissolved in 30 mL of toluene. The reaction flask is charged with C_2H_2 (300 torr) and H_2 (300 torr) and heated to 80 °C.

Water-Gas Shift. Method A. $[Rh_2(\mu\text{-}H)(\mu\text{-}CO)(CO)_2(dpm)_2]^+$-$p\text{-}CH_3C_6H_4SO_3^-$, 0.05 g, is dissolved in 50 mL of 1-propanol, and an aqueous solution, 2 mL, containing 2 molar equiv of a salt such as LiCl is added. The solution is placed under CO (500 torr) and heated to 90 °C.

Method B. $[Rh_2(\mu\text{-}CO)(CO)_2(dpm)_2]$, 0.075 g, is dissolved in 50 mL of bis(2-ethoxyethyl) ether, and 0.01 g of *p*-toluenesulfonic acid dissolved in 2 mL of H_2O is added. The solution is placed under CO (500 torr) and heated to 90 °C.

Hydroformylation Using CO + H_2O. $[Rh_2(\mu\text{-}CO)(CO)_2(dpm)_2]$, 0.05 g, is dissolved in 30 mL of 1-propanol, bis(2-ethoxyethyl) ether, or *p*-dioxane containing 2 molar equiv of LiCl, 1 molar equiv of *p*-toluenesulfonic acid, and 2 mL of H_2O. The system is charged with CO (300 torr) and C_2H_4 (300 torr) and heated to 90 °C.

Data Collection and Reduction. Dark green crystals of $[Rh_2(\mu\text{-}H)(\mu\text{-}CO)(CO)_2(dpm)_2]^+(p\text{-}CH_3C_6H_4SO_3)^-\cdot 2THF$ were obtained as above. The crystals showed no signs of decomposition after exposure to air for a period of 2 weeks, and protection of the crystal chosen for data collection from the atmosphere was deemed unnecessary. On the basis of optical goniometry and precession photographs, it was determined that the crystals belong to the monoclinic system. The observed systematic absence of hkl, $h + k = 2n + 1$, is consistent with space groups $C2$ (C_2^3), Cm (C_s^3), and $C2/m$ (C_{2h}^3).[23] The lattice constants at 24 °C were determined from a least-squares refinement of 12 intense, high-angle reflections ($(\sin\theta)/\lambda \geq 0.1528$)[24] on a Picker FACS-1 diffractometer equipped with a graphite monochromator using Mo K$\bar{\alpha}$ radiation (λ = 0.710 69 Å). The lattice constants are a = 24.391 (11) Å, b = 18.863 (9) Å, c = 14.440 (6) Å, and β = 107.81 (2)°. The calculated density (Z = 4) of 1.44 g/cm^3 agrees with a value of 1.42 (2) g/cm^3 determined by the flotation method.

The mosaicity of the crystal used for intensity measurements was examined by means of a narrow-source, open-counter ω-scan technique.[25] The full widths at half-maximum for typical strong reflections were ≤0.12°. Intensities were measured by the θ–2θ scan technique. The crystal was mounted with the b^* axis offset by 3.5° from the ϕ axis of the diffractometer. The takeoff angle for the X-ray tube was 1.4°. The scan was from 0.6° below the Kα_1 peak to 0.6° above the Kα_2 peak. The scan speed was 1°/min, and backgrounds were counted at each end of the scan range for 10 s ($2\theta \leq 35°$) or 20 s ($35° < 2\theta \leq 40°$). Attenuator foils were automatically inserted when the intensity of the diffracted beam reached 10 000 counts/s. The pulse-height

(23) "International Tables for X-ray Crystallography"; Kynoch Press: Birmingham, England, 1960; Vol. I, pp 81, 87, 95.
(24) The programs for refinement of lattice constants and automated operation of the diffractometer are those of Busing and Levy as modified by Picker Corp.
(25) Furnas, T. C. "Single Crystal Orienter Instruction Manual"; General Electric Co.: Milwaukee, WI, 1957; Chapter 10.

Table I. Final Positional and Thermal Parameters for $[Rh_2(\mu\text{-}H)(\mu\text{-}CO)(CO)_2(dpm)_2]^+CH_3C_6H_4SO_3^-\cdot 2THF$

	x	y	z	β_{11}[a]	β_{22}	β_{33}	β_{12}	β_{13}	β_{23}
Rh(1)	0.29491 (5)	0.0 (0)	0.20087 (9)	15.0 (4)	26.6 (6)	49.7 (10)	0.0 (0)	6.2 (4)	0.0 (0)
Rh(2)	0.17808 (5)	0.0 (0)	0.12623 (10)	14.9 (4)	22.2 (6)	57.8 (11)	0.0 (0)	10.7 (4)	0.0 (0)
S	0.24138 (25)	0.500 000 (0)	0.1809 (4)	29.6 (15)	60.6 (28)	67. (4)	0.0 (0)	14.6 (20)	0.0 (0)
P(1)	0.30238 (12)	−0.119 49 (18)	0.180 44 (21)	15.3 (7)	29.4 (13)	50.5 (22)	1.6 (7)	8.4 (9)	0.7 (12)
P(2)	0.17406 (12)	0.117 86 (16)	0.083 28 (22)	14.9 (7)	26.3 (13)	54.1 (22)	−0.6 (7)	8.7 (10)	1.6 (13)
O(PTS1)	0.2304 (5)	0.4364 (6)	0.1226 (8)	42. (3)	92 (6)	130 (10)	−10 (4)	29 (5)	−64 (6)
O(PTS2)	0.2965 (6)	0.500 000 (0)	0.2544 (9)	31. (4)	69 (7)	73 (10)	0.0 (0)	7 (5)	0.0 (0)
C(DPM)	0.2437 (4)	−0.1490 (6)	0.0712 (7)	9.7 (22)	41 (5)	37 (7)	0.9 (27)	3 (3)	−6 (5)
C(1)	0.3680 (9)	0.0 (0)	0.2943 (14)	21. (5)	48 (9)	75 (15)	0.0 (0)	1 (7)	0.0 (0)
O(1)	0.4134 (7)	0.0 (0)	0.3475 (12)	27. (4)	64 (8)	140 (15)	0.0 (0)	−21 (6)	0.0 (0)
C(2)	0.1000 (8)	0.0 (0)	0.1089 (14)	23. (5)	24 (7)	89 (15)	0.0 (0)	13 (7)	0.0 (0)
O(2)	0.0520 (6)	0.0 (0)	0.1032 (12)	18. (3)	55 (7)	174 (15)	0.0 (0)	26 (6)	0.0 (0)
C(3)	0.2276 (7)	0.0 (0)	0.2760 (14)	15. (4)	39 (8)	61 (14)	0.0 (0)	8 (6)	0.0 (0)
O(3)	0.2231 (6)	0.0 (0)	0.3505 (10)	34. (4)	82 (8)	51 (9)	0.0 (0)	22 (5)	0.0 (0)
O(THF1)	0.4274 (19)	0.500 000 (0)	−0.378 (3)	150. (22)	143 (21)	358 (63)	0.0 (0)	36 (29)	0.0 (0)
C(THF1)	0.4115 (15)	0.4383 (11)	−0.4322 (20)	131. (14)	46 (8)	134 (20)	−10 (9)	4 (14)	−4 (11)
C(THF1)	0.3951 (17)	0.4636 (13)	−0.5196 (18)	182. (17)	93 (18)	133 (21)	12 (12)	−53 (16)	−33 (14)
O(THF2)	0.0 (0)	0.3338 (20)	−0.500 000 (0)	115. (25)	116 (22)	364 (52)	0.0 (0)	17 (29)	0.0 (0)
C(THF2)	0.0375 (18)	0.2880 (23)	−0.535 (4)	47. (9)	176 (33)	291 (41)	17 (18)	71 (15)	57 (44)
C(THF2)	0.0216 (24)	0.2289 (17)	−0.513 (6)	104. (35)	120 (20)	490 (98)	46 (24)	145 (38)	10 (58)
C(PTS)	0.0561 (14)	0.500 000 (0)	0.3861 (24)	15.2 (11)					
H	0.236 (5)	0.0 (0)	0.079 (8)	3.5 (29)					

[a] The form of the anisotropic thermal ellipsoid is $\exp[-(h^2\beta_{11} + k^2\beta_{22} + l^2\beta_{33} + 2hk\beta_{12} + 2hl\beta_{13} + 2kl\beta_{23})]$. Entries are $\times 10^4$.

Table II. Group Parameters[a]

	x_c	y_c	z_c	ϕ	θ	ρ
P1C1	0.420 93 (25)	−0.140 74 (29)	0.1330 (4)	−2.565 (8)	−2.286 (5)	−2.375 (7)
P1C2	0.301 29 (19)	−0.2324 (3)	0.3444 (4)	−3.190 (6)	2.422 (5)	1.576 (6)
P2C1	0.140 82 (20)	0.2347 (3)	0.2157 (4)	2.957 (7)	−2.385 (5)	1.218 (6)
P2C2	0.081 46 (26)	0.1284 (3)	−0.1269 (5)	1.051 (7)	−2.446 (5)	−1.937 (7)
tol	0.147 2 (4)	0.500 00 (0)	0.2888 (7)	1.570 80 (0)	−0.768 (9)	−1.570 80 (0)

[a] x_c, y_c, and z_c are the groups' center of mass coordinates; ϕ, θ, and ρ are angular parameters described previously. B (in Å^2), the group thermal parameter which was not refined, is 0.0.

analyzer was set for a 90% window centered on Mo Kα radiation.

Data were collected from the quadrant with $h, k \geq 0$ in the range $3.5° \leq 2\theta \leq 40°$. Three standard reflections were monitored every 100 observations. The intensities of the standards varied by ca. ±7% but showed no significant trends over the course of data collection. A total of 3187 reflections were observed. The values of I and $\sigma^2(I)$ were obtained from expressions described previously[26] and converted to F^2 and $\sigma^2(F^2)$ by application of Lorentz and polarization corrections. The value of p used in the expression for the variance was 0.04.[27] The approximate dimensions of the crystal were 0.32 × 0.21 × 0.08 mm. The linear absorption coefficient for Mo Kα radiation is 6.97 cm^{-1}, and no correction for absorption was made. The final data set consisted of 3187 reflections of which 2194 had $F_o^2 \geq 3\sigma(F_o^2)$.

Solution and Refinement of the Structure. The structure was solved by standard heavy-atom methods in the space group $C2/m$.[28] The positions of two rhodium atoms on the crystallographic mirror plane at $y = 0$ were determined from a three-dimensional Patterson map as were the positions of two phosphorus atoms.

Refinement of the scale factor and atomic positional and thermal parameters for these atoms resulted in residuals of $R_1 = 0.3238$ and $R_2 = 0.4102$.[29] In this and all subsequent refinements, the quantity minimized was $\sum w(|F_o| - |F_c|)^2$ where the weights, w, were $4F^2/\sigma^2(F^2)$. Only those reflections with $F_o^2 \geq 3\sigma(F_o^2)$ were included in the refinements. Scattering factors for neutral Rh, S, P, O, and C were those tabulated by Cromer and Mann.[30] The effects of anomalous dispersion were included in the calculation of $|F_c|$; values of $\Delta f'$ and $\Delta f''$ were those of Cromer and Liberman.[31] The scattering factors for hydrogen were those of Stewart et al.[32]

The remaining atoms were located by the usual sequence of difference Fourier maps and least-squares refinements. In these refinements the bis(diphenylphosphino)methane and p-toluenesulfonate phenyl rings were treated as rigid groups[33] with d(C–C) = 1.392 Å. A model in which the carbon and oxygen atoms were refined with isotropic thermal parameters and all other atoms with anisotropic parameters was refined to convergence with residuals $R_1 = 0.0643$ and $R_2 = 0.0789$. The third most intense peak of the subsequent difference Fourier map corresponded to the hydride with its y coordinate fixed on the mirror plane at $y = 0$. Most other peaks in the Fourier map including the highest one corresponded to phenyl hydrogen atoms.

The two THF solvent molecules showed extremely large thermal motion when refined with isotropic thermal parameters, with B values ranging from 9 to 25 Å^2. A difference Fourier synthesis following a refinement of the THF atomic positions with fixed thermal parameters, $B = 12.0$ Å^2, did not show any peaks which could be logically incorporated into a static disorder model. In the final model, all nongroup, nonhydrogen atoms including those of the two THF molecules were refined with anisotropic thermal parameters. The dpm phenyl hydrogen atoms were included in the rigid groups with isotropic thermal parameters constrained to $B_H = B_C + 1$. The total of 208 variables for 2123 independent observations was refined to convergence with residuals of $R_1 = 0.0578$ and $R_2 = 0.0698$. In the final cycle of refinement none of the parameters for the $[Rh_2(\mu\text{-}H)(\mu\text{-}CO)(CO)_2(dpm)_2]^+$ unit or p-toluenesulfonate shifted by more

(26) Goldberg, S. Z.; Kubiak, C.; Meyer, C. D.; Eisenberg, R. *Inorg. Chem.* **1975**, *14*, 1650.
(27) Corfield, P. W. R.; Doedens, R. J.; Ibers, J. A. *Inorg. Chem.* **1967**, *6*, 197.
(28) All computations were performed on an IBM 3032 computer. The data processing program was an extensively modified version of Raymond's URFACS. In addition, local versions of the following were used: Ibers' NUCLS, a group least-squares program; Zalkin's FORDAP Fourier program; ORFFE, a function and error program by Busing, Martin, and Levy; Johnson's ORTEP thermal ellipsoid plotting program.
(29) $R_1 = \sum||F_o| - |F_c||/\sum|F_o|$. $R_2 = [\sum w(|F_o| - |F_c|)^2/\sum w|F_o|^2]^{1/2}$. The estimated standard deviation of an observation of unit weight is given by $[\sum w(|F_o| - |F_c|)^2/(N_o - N_v)]^{1/2}$, where N_o and N_v are the number of observations and variables, respectively.
(30) Cromer, D. T.; Mann, B. *Acta Crystallogr., Sect. A* **1968**, *24A*, 321.
(31) Cromer, D. T.; Liberman, D. *J. Chem. Phys.* **1970**, *53*, 1891.
(32) Stewart, R. F.; Davidson, E. R.; Simpson, W. T. *J. Chem. Phys.* **1965**, *42*, 3175.
(33) (a) Eisenberg, R.; Ibers, J. A. *Inorg. Chem.* **1965**, *4*, 773. (b) LaPlaca, S. J.; Ibers, J. A. *J. Am. Chem. Soc.* **1965**, *87*, 2851. (c) LaPlaca, S. J.; Ibers, J. A. *Acta Crystallogr.* **1965**, *18*, 511.

Table III. Derived Positional and Thermal Parameters of Group Atoms

	x	*y*	*z*	*B*, Å²
P1C11[a]	0.367 60 (28)	−0.1373 (4)	0.1493 (6)	3.88 (25)
P1C12	0.3757 (3)	−0.1039 (4)	0.0685 (5)	6.3 (3)
P1C13	0.4290 (4)	−0.1073 (5)	0.0523 (5)	7.7 (4)
P1C14	0.474 26 (28)	−0.1441 (5)	0.1168 (7)	6.1 (3)
P1C15	0.4661 (3)	−0.1776 (5)	0.1975 (6)	8.1 (4)
P1C16	0.4128 (4)	−0.1742 (4)	0.2138 (5)	6.8 (3)
P1H12	0.3443 (4)	−0.0787 (6)	0.0245 (7)	7.3
P1H13	0.4346 (6)	−0.0845 (6)	−0.0029 (7)	8.7
P1H14	0.5107 (3)	−0.1465 (7)	0.1056 (9)	7.1
P1H15	0.4970 (4)	−0.2027 (7)	0.2415 (8)	9.1
P1H16	0.4073 (5)	−0.1970 (6)	0.2689 (7)	7.8
P1C21	0.3029 (3)	−0.1838 (4)	0.2728 (5)	3.61 (24)
P1C22	0.3040 (3)	−0.1601 (3)	0.3646 (6)	5.30 (29)
P1C23	0.3024 (3)	−0.2087 (5)	0.4363 (4)	7.2 (4)
P1C24	0.2997 (4)	−0.2810 (4)	0.4161 (6)	6.2 (3)
P1C25	0.2986 (4)	−0.3047 (3)	0.3242 (7)	7.5 (4)
P1C26	0.3002 (3)	−0.2561 (4)	0.2526 (5)	6.0 (3)
P1H22	0.3059 (5)	−0.1107 (3)	0.3784 (8)	6.3
P1H23	0.3031 (5)	−0.1925 (7)	0.4990 (5)	8.2
P1H24	0.2985 (5)	−0.3142 (6)	0.4650 (7)	7.2
P1H25	0.2967 (6)	−0.3541 (3)	0.3104 (9)	8.5
P1H26	0.2995 (5)	−0.2723 (6)	0.1899 (6)	7.0
P2C11	0.1541 (3)	0.1833 (4)	0.1568 (5)	4.28 (26)
P2C12	0.1544 (4)	0.2547 (5)	0.1325 (5)	7.5 (4)
P2C13	0.1411 (4)	0.3062 (3)	0.1915 (7)	8.4 (4)
P2C14	0.1276 (4)	0.2862 (4)	0.2747 (6)	6.9 (4)
P2C15	0.1273 (3)	0.2148 (5)	0.2989 (5)	6.8 (4)
P2C16	0.1405 (3)	0.1633 (3)	0.2400 (6)	4.47 (26)
P2H12	0.1636 (5)	0.2684 (7)	0.0758 (6)	8.5
P2H13	0.1413 (6)	0.3549 (4)	0.1749 (10)	9.4
P2H14	0.1185 (5)	0.3213 (5)	0.3149 (8)	7.9
P2H15	0.1180 (5)	0.2011 (7)	0.3557 (6)	7.8
P2H16	0.1403 (5)	0.1146 (4)	0.2565 (8)	5.47
P2C21	0.1233 (3)	0.1294 (5)	−0.0362 (5)	4.53 (27)
P2C22	0.136 96 (29)	0.1045 (5)	−0.1172 (6)	6.1 (3)
P2C23	0.0952 (4)	0.1035 (5)	−0.2079 (5)	7.8 (4)
P2C24	0.0397 (3)	0.1274 (5)	−0.2176 (5)	7.3 (4)
P2C25	0.025 97 (28)	0.1523 (5)	−0.1367 (7)	8.9 (4)
P2C26	0.0678 (4)	0.1533 (5)	−0.0459 (6)	7.6 (4)
P2H22	0.1748 (3)	0.0882 (7)	−0.1105 (9)	7.1
P2H23	0.1045 (6)	0.0865 (7)	−0.2632 (7)	8.8
P2H24	0.0112 (5)	0.1267 (7)	−0.2796 (6)	8.3
P2H25	−0.0119 (3)	0.1686 (7)	−0.1433 (10)	9.9
P2H26	0.0584 (6)	0.1702 (7)	0.0093 (7)	8.6
S1C11	0.1888 (5)	0.50	0.2409 (10)	5.0 (3)
S1C12	0.1307 (6)	0.50	0.1876 (7)	6.2 (3)
S1C13	0.0890 (4)	0.50	0.2354 (11)	7.5 (4)
S1C14	0.1055 (7)	0.50	0.3366 (11)	9.6 (5)
S1C15	0.1637 (8)	0.50	0.3900 (7)	9.8 (5)
S1C16	0.2054 (5)	0.50	0.3422 (10)	9.1 (5)

[a] In the numbering scheme for phenyl carbons, the first number following P or S denotes the phosphorus or sulfur atom to which the ring is bound. The first number following C is an identifier for the phenyl rings bound to the same phosphorus. The last number always denotes the position of the carbon in the ring with C1 bound to phosphorus or sulfur. Phenyl hydrogen atoms are numbered the same as the carbon to which they are bound.

than 12% of their estimated standard deviations. Several of the thermal parameters for the THF atoms shifted by as much as 1 estimated standard deviation. The final estimated standard deviation for an observation of unit weight was 2.24 e. The largest peak of a final difference Fourier map was 0.6 e/Å or 34% of a typical carbon atom peak in this study.

The final atomic positional and thermal parameters are given in Table I. Group parameters are given in Table II. Derived positional and thermal parameters for the group atoms are given in Table III. A listing of observed and calculated structure factors is available as supplementary material.

Results and Discussion

Preparation of Binuclear Rh(0) A-Frame Precursors. The Rh(0) species $[Rh_2(CO)_2(dpm)_2]$ is prepared by borohydride reduction of $[Rh_2Cl_2(CO)_2(dpm)_2]$. The complex exhibits a single ν(CO) at 1915 cm^{-1} and does not show peaks which might be attributed to ν(Rh–H). There is no spectroscopic evidence for a possible hydride formulation. The substitution of $NaBD_4$ as the reducing agent has no effect on the IR spectrum, and the ^1H NMR spectrum in the hydride region, upfield of Me_4Si to −30 ppm, is silent. The $^{31}P\{^1H\}$ NMR spectrum is complicated, showing a symmetric multiplet centered at δ 29.51, with four principal lines. The spectrum is qualitatively different from those of other binuclear dpm-bridged Rh complexes which generally display two intense principal lines separated, to first order, by $^1J_{Rh-P}$.[3,8] We propose the identity of the complex as the metal–metal-bonded Rh(0) dimer II, which is consistent with the spectroscopic data and which is strongly supported by its reaction chemistry (vide infra).

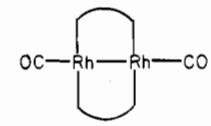

II

A second, related Rh(0) complex is prepared by the reaction of $RhH(CO)(PPh_3)_3$ with bis(diphenylphosphino)methane (dpm). A stoichiometric quantity of H_2 is produced during the reaction, according to eq 3. The complex in solution

$$2RhH(CO)(PPh_3)_3 + 2dpm \rightleftharpoons [Rh_2(CO)_2(dpm)_2] + 6PPh_3 + H_2 \quad (3)$$

differs from that prepared by borohydride reduction of $[Rh_2Cl_2(CO)_2(dpm)_2]$ in color and by the appearance of both a bridging and a terminal ν(CO), 1800 s, br and 1936 cm^{-1}, respectively (CH_2Cl_2 solution), in the IR spectrum. This difference relates to the presence of triphenylphosphine which is liberated during the reaction. The predominant species in solution appears to be $[Rh_2(\mu\text{-}CO)(CO)(dpm)_2(PPh_3)]$. Evidence for a coordinated triphenylphosphine is found in the $^{31}P\{^1H\}$ NMR. A broadened doublet at δ 39.35 is assigned to bound PPh_3, while two complex multiplets at δ 19.35 and 9.40 are assigned to two chemically different pairs of dpm phosphorus nuclei. Free triphenylphosphine is also seen at δ −8.47 (s). Identical IR and NMR data are obtained when triphenylphosphine is added to a solution of $[Rh_2(CO)_2(dpm)_2]$. Hence in solution, the product of the reaction of $RhH(CO)(PPh_3)_3$ with dpm is $[Rh_2(\mu\text{-}CO)(CO)(dpm)_2(PPh_3)]$, a triphenylphosphine adduct of $[Rh_2(CO)_2(dpm)_2]$. Surprisingly, the triphenylphosphine appears only weakly bound and is easily replaced. Microanalytical data for the isolated solid indicates the replacement of PPh_3 by 1 molecule of solvent. The presence of the solvent molecule is verified by ^1H NMR data. The solid samples of the complex which have been isolated are formulated as solvated isomers of $[Rh_2(CO)_2(dpm)_2]$, i.e., $[Rh_2(\mu\text{-}CO)(CO)(dpm)_2(Sol)]$ (Sol = CH_2Cl_2, THF). The strongest evidence for this formulation comes from the fact that while their IR and NMR spectra are different, the two Rh(0) complexes $[Rh_2(CO)_2(dpm)_2]$ and $[Rh_2(\mu\text{-}CO)(CO)(dpm)_2(Sol)]$ undergo addition reactions with small molecules to give identical products which are described below.

Additions of CO and H^+ and the Synthesis of $[Rh_2(\mu\text{-}H)(\mu\text{-}CO)(CO)_2(dpm)_2]^+$. The complex $[Rh_2(CO)_2(dpm)_2]$ exhibits an extensive small molecule addition chemistry. The reaction with CO is accompanied by a rapid solution color change to red-orange after which $[Rh_2(\mu\text{-}CO)(CO)_2(dpm)_2]$ may be isolated in analytically pure form. The IR spectrum shows a bridging carbonyl stretch at 1835 cm^{-1} in addition to terminal stretches at 1940 s, sh and 1920 vs. The controlled addition of CO to $[Rh_2(CO)_2(dpm)_2]$ by gas syringe followed by GC monitoring of the reaction shows that 1 equiv of CO

is consumed; no H_2 is produced. The ^1H NMR spectrum of $[Rh_2(\mu\text{-}CO)(CO)_2(dpm)_2]$ displays no resonances attributable to a Rh hydride formulation. The $^{31}P\{^1H\}$ NMR indicates a symmetric phosphorus environment, and is shown in Figure 4. Protonation of $[Rh_2(CO)_2(dpm)_2]$ with 1 equiv of a noncoordinating acid, HA ($A^- = p\text{-}CH_3C_6H_4SO_3^-$ or PF_6^-), leads to $[Rh_2(H)(CO)_2(dpm)_2]^+A^-$. Only a trace of H_2 is observed in the course of the reaction. The protonated complex has not yet been isolated in pure form but has been characterized in solution. The ^1H NMR spectrum reveals a featureless hydride resonance at δ −10.1, and in the IR, two ν(CO) are seen at 1974 s,sh and 1951 vs cm^{-1} (THF solution).

We conclude that the products are A-frame complexes with the added proton or CO in the bridgehead position. The identities of the products of carbonylation and protonation of $[Rh_2(CO)_2(dpm)_2]$ as μ-CO and μ-H A-frame complexes, respectively, gain additional support from their reactions which lead to a μ-hydride, μ-carbonyl derivative, $[Rh_2(\mu\text{-}H)(\mu\text{-}CO)(CO)_2(dpm)_2]^+$. This common derivative is formed either by protonation of $[Rh_2(\mu\text{-}CO)(CO)_2(dpm)_2]$ or by addition of CO to $[Rh_2(H)(CO)_2(dpm)_2]^+$. These reactions are reversible. Heating $[Rh_2(\mu\text{-}H)(\mu\text{-}CO)(CO)_2(dpm)_2]^+$ under N_2 regenerates $[Rh_2(H)(CO)_2(dpm)_2]^+$, while addition of 1 equiv of $NaHB(OMe)_3$ to the complex yields $[Rh_2(\mu\text{-}CO)(CO)_2(dpm)_2]$ and 1 equiv of H_2. The μ-hydride, μ-carbonyl complex exhibits ν(CO) at 1972 s, 1957 vs, and 1870 s cm^{-1}, and a broad hydride resonance at δ −9.71. The $^{31}P\{^1H\}$ NMR of the complex suggests a symmetric phosphorus environment, and is shown in Figure 5. The structure of the *p*-toluenesulfonate salt of the complex has been determined by X-ray crystallography and is described below in the discussion of the solid-state structure as a μ-hydride A-frame of Rh(I) with a carbon monoxide bound in the endo pocket. The reversible carbonylation of $[Rh_2(H)(CO)_2(dpm)_2]^+$ to $[Rh_2(\mu\text{-}H)(\mu\text{-}CO)(CO)_2(dpm)_2]^+$ points to the identity of the former complex as a μ-hydride A-frame of Rh(I). The reversible carbonylation is analogous to that reported for the structurally similar A-frame CO adducts $[Rh_2(\mu\text{-}Cl)(\mu\text{-}CO)(CO)_2(dpm)_2]^+$[3] and $[Rh_2(\mu\text{-}S)(\mu\text{-}CO)(CO)_2(dpm)_2]$.[6]

The spectroscopic data for $[Rh_2(\mu\text{-}CO)(CO)_2(dpm)_2]$ together with its facile protonation to form $[Rh_2(\mu\text{-}H)(\mu\text{-}CO)(CO)_2(dpm)_2]^+$ provides compelling evidence of a Rh(0) carbonyl-bridged A-frame complex, analogous to Pd(I), Pt(I), and Rh species reported previously.[2,8b,14,16,18] The μ-hydride, μ-carbonyl complex may thus be viewed as resulting from either the introduction of CO into the pocket of the hydride A-frame or from protonation of the neutral Rh(0) carbonyl A-frame. The reactions interrelating the hydride- and carbonyl-bridged complexes are summarized in Scheme I.

Solid-State Structure of $[Rh_2(\mu\text{-}H)(\mu\text{-}CO)(CO)_2(PPh_2CH_2PPh_2)_2]^+p\text{-}CH_3C_6H_4SO_3^-\cdot 2THF$

The crystal structure is composed of discrete $[Rh_2(\mu\text{-}H)(\mu\text{-}CO)(CO)_2(dpm)_2]^+$ cations, $p\text{-}CH_3C_6H_4SO_3^-$ anions, and THF solvent molecules. The asymmetic unit contains half of the complex. The present structure determination of the complex represents our fourth attempt and first success. The structures of the hexafluorophosphate, tetrafluoroborate, and trifluoromethylsulfonate salts were found in earlier studies to be badly disordered and intractable.

The molecular structure of $[Rh_2(\mu\text{-}H)(\mu\text{-}CO)(CO)_2(dpm)_2]^+$ consists of two rhodium atoms bridged by two bis(diphenylphosphino)methane ligands, a hydride, and a carbon monoxide. Each of the two molecular ions and two THF solvent molecules possess an element of crystallographic symmetry. The $[Rh_2(\mu\text{-}H)(\mu\text{-}CO)(CO)_2(dpm)_2]^+$ cation is bisected by a mirror plane which contains the two rhodium atoms, bridging hydride, and bridging and terminal carbonyls. The *p*-toluenesulfonate anion also lies on a mirror plane, while the two THF molecules possess twofold and mirror symmetry, respectively. Figure 1 presents a perspective view of the $[Rh_2(\mu\text{-}H)(\mu\text{-}CO)(CO)_2(dpm)_2]^+$ cation in which the phenyl rings have been omitted. A second view, with phenyl rings, appears in Figure 2. A stereoview of the unit cell contents is given in Figure 3. Interatomic distances and angles are listed in Table IV.

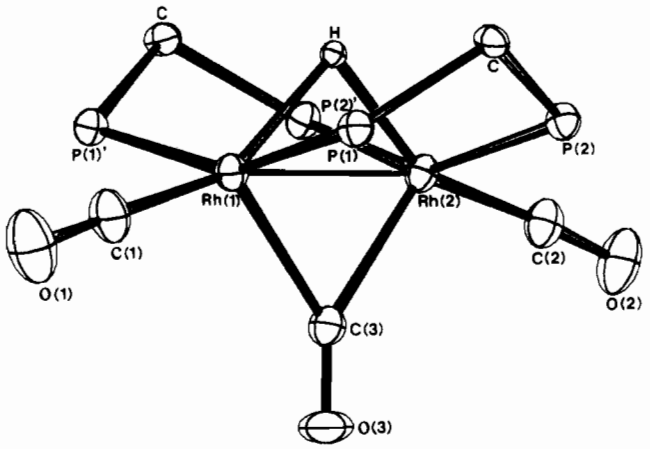

Figure 1. Perspective view of the cation $[Rh_2(\mu\text{-}H)(\mu\text{-}CO)(CO)_2(dpm)_2]^+$ in which phenyl rings have been omitted for clarity.

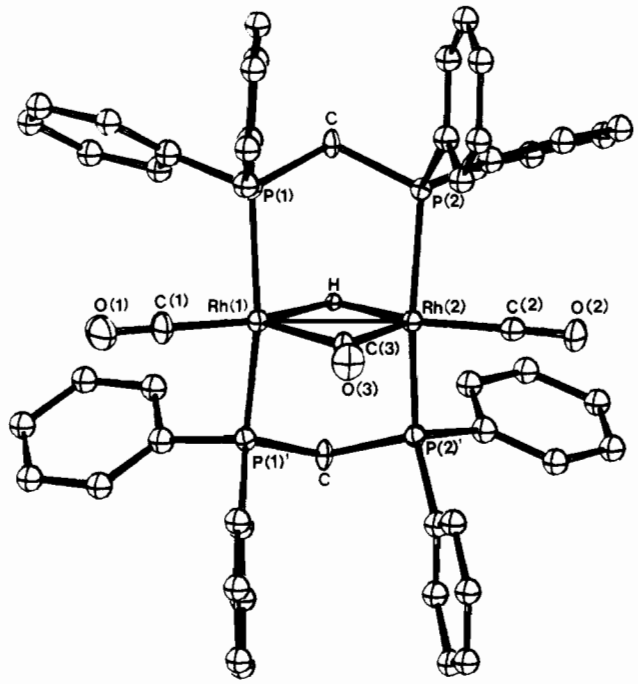

Figure 2. Perspective view of the cation $[Rh_2(\mu\text{-}H)(\mu\text{-}CO)(CO)_2(dpm)_2]^+$.

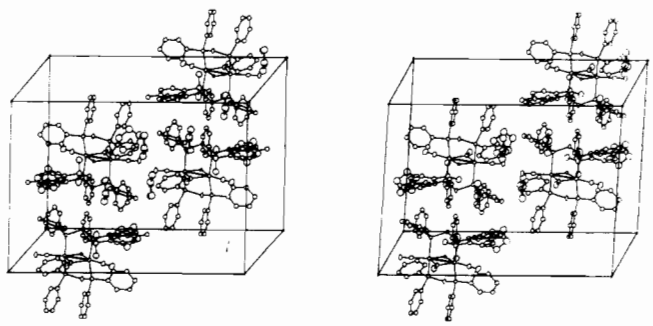

Figure 3. Stereoview of the unit cell of $[Rh_2(\mu\text{-}H)(\mu\text{-}CO)(CO)_2(dpm)_2]^+(p\text{-}CH_3C_6H_4SO_3)^-\cdot 2THF$.

Scheme I

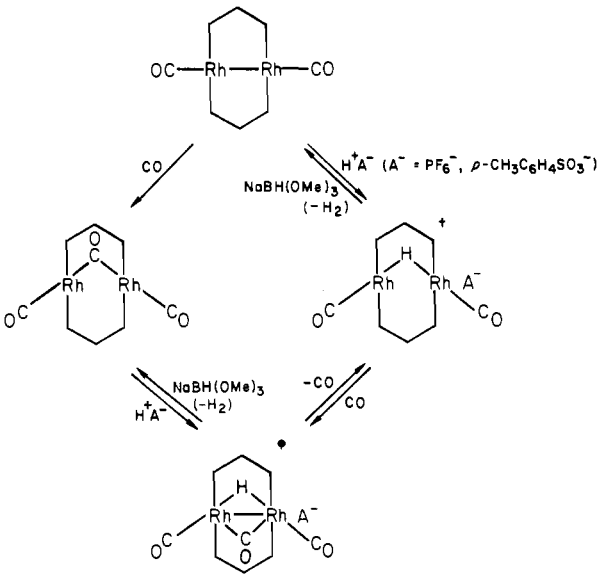

The coordination geometry about each rhodium atom is distorted square pyramidal. The approximately square basal planes contain two trans dpm phosphorus atoms, a terminal carbon monoxide, and the shared corner corresponding to the bridging hydride. These ligand atoms exhibit trans angles of P(1)–Rh(1)–P(1)′ = 155.2 (2)° and H–Rh(1)–C(1) = 155(4)° at Rh(1) and P(2)–Rh(2)–P(2)′ = 149.9 (2)° and H–Rh(2)–C(2) = 151 (3)° at the second rhodium atom, Rh(2). The corresponding cis angles exhibited by the basal ligands are P(1)–Rh(1)–H = 84.6 (8)°, P(1)–Rh(1)–C(1) = 90.4 (2)°, P(2)–Rh(2)–H = 82.5 (7)°, and P(2)–Rh(2)–C(2) = 90.4 (2)° at Rh(1) and Rh(2), respectively. The rhodium atoms, Rh(1) and Rh(2), are displaced from their basal planes of ligands by 0.476 (3) and 0.564 (3) Å. The bridging carbon monoxide is mutually apical, showing cis angles to the two sets of basal ligands of C(3)–Rh(1)–H = 90 (4)°, C(3)–Rh(1)–P(1) = 101.1 (1)°, and C(3)–Rh(1)–C(1), 114.6 (9)° at Rh(1) and C(3)–Rh(2)–H = 97 (3)°, C(3)–Rh(2)–P(2) = 103.75 (9°), and C(3)–Rh(2)–C(2) = 112.3 (8)° at Rh(2). The dihedral angle between the least-square planes [H,C(1),P(1),P(1)′] and [H,C(2),P(2),P(2)′] is 114.6°.

The Rh–Rh separation of 2.731 (2) Å is well within the range normally reported for Rh–Rh single bonds.[34-38] The compression along the Rh–Rh internuclear axis is evident in a shorter separation between the metals than between the adjacent dpm phosphorus atoms, P(1)···P(2), 3.012 (4) Å. The bridging hydride bond lengths, Rh(1)–H = 1.97 (11) and Rh(2)–H = 1.75 (11) Å, are within the range usually found for μ-hydrido complexes of second- and third-row group 8 transition metals.[39] The $[Rh_2(\mu\text{-H})(\mu\text{-CO})(CO)_2(dpm)_2]^+$ cation shows the structural arrangement of a hydride bridged A-frame complex with a CO molecule bound in the endo pocket. The structure bears a strong resemblance to two other endo A-frame CO adducts $[Rh_2(\mu\text{-Cl})(\mu\text{-CO})(CO)_2(dpm)_2]^+$[3,5] and $[Ir_2(\mu\text{-S})(\mu\text{-CO})(CO)_2(dpm)_2]$.[6] This resemblance is unexpected in view of the usual electron-counting formalisms which acknowledge bridging H, S, and Cl atoms as 1-, 2-, and 3-e donors, respectively. Thus, the electron count for the μ-H structure is implied to be 2 e less than the μ-Cl and μ-S structures. The apparent differences between the three structures, however, are small. The present structure does show a slightly shorter M–M distance of *d*(Rh–Rh) = 2.731 (2) Å compared to $[Rh_2(\mu\text{-Cl})(\mu\text{-CO})(CO)_2(dpm)_2]^+$, *d*(Rh–Rh) = 2.8415 (7) Å, and $[Ir_2(\mu\text{-S})(\mu\text{-CO})(CO)_2(dpm)_2]$, *d*(Ir–Ir) = 2.843 (2) Å. The angle through the bridgehead ligand is also wider, Rh–H–Rh = 94 (5)°, than in the μ-Cl and μ-S structures, Rh–Cl–Rh = 66.51 (4)° and Ir–S–Ir = 70.5 (1)°. The wider bond angle, however, is expected from shorter Rh–H bond lengths: 1.97 (11) and 1.75 (11) Å compared to Rh–Cl = 2.572 (2), 2.607 (2) and Ir–S = 2.463 (3) Å. While we offer no bonding description to account for the structural similarity of the μ-H complex to the μ-Cl and μ-S species, we note that Hoffman and Hoffmann have found the molecular orbital energy levels in $[Rh_2(\mu\text{-Cl})(\mu\text{-CO})(CO)_2(dpm)_2]^+$ and $[Rh_2(\mu\text{-H})(\mu\text{-CO})(CO)_2(dpm)_2]^+$ to be qualitatively very similar.[40] An analogous trend in a series of $(\mu\text{-H})Os_3(CO)_{10}(\mu\text{-L})$ structures (L = H, Cl, Br) has been reported by Churchill.[39b] The substitution of L = H for Cl or Br in these complexes has been found to lead to no significant changes in the overall structure except a contraction of the bridged Os–Os bond, *d*(Os–Os) = 2.683 (1) for L = H compared to 2.846 (1) for L = Cl and 2.851 (1), 2.876 (1) Å for L = Br.

The remainder of bond distances for $[Rh_2(\mu\text{-H})(\mu\text{-CO})(CO)_2(dpm)_2]^+$ and the *p*-toluenesulfonate anion appear normal. The two Rh–P bond lengths of 2.301 (3) and 2.317 (4) Å agree with values reported for similar rhodium dpm complexes.[3,5,9] The Rh–C distances for the terminal, 1.83 (2) and 1.84 (2) Å, and bridging carbonyls, 2.15 (2) and 2.13 (2)

Table IV. Bond Distances (Å) and Angles (Deg) for $[Rh_2(\mu\text{-H})(\mu\text{-CO})(CO)_2(dpm)_2]^+(p\text{-}CH_3C_6H_5SO_3)^-\cdot 2THF$

Rh(1)–C(1)	1.83 (2)	P(1)–P1C21	1.792 (8)
Rh(1)–H	1.97 (11)	P(1)–P1C11	1.810 (8)
Rh(1)–C(3)	2.15 (2)	P(2)–P2C11	1.790 (9)
Rh(1)–P(1)	2.317 (4)	P(2)–P2C21	1.803 (7)
Rh(1)–Rh(2)	2.731 (2)	P(1)···P(2)	3.012 (4)
Rh(2)–H	1.75 (11)	S–O(PTS1)	1.44 (1)
Rh(2)–C(2)	1.84 (2)	S–O(PTS2)	1.44 (1)
Rh(2)–C(3)	2.13 (2)	S–S1C11	1.75 (1)
Rh(2)–P(2)	2.301 (3)	C(PTS)–S1C14	1.58 (4)
P(1)–C(dpm)	1.86 (1)	O(PTS1)···P1H12	2.36 (1)
P(2)–C(dpm)	1.86 (1)	O(PTS1)···P2H22	2.41 (2)
C(1)–O(1)	1.14 (2)	P1H13···P1H14	2.56 (2)
C(2)–O(2)	1.15 (2)	P1H16···P1C21	2.57 (2)
C(3)–O(3)	1.11 (2)	P2H25···P2H26	2.52 (2)
C(1)–Rh(1)–H	155 (4)	P2C11–(2)–P2C21	104.6 (4)
C(1)–Rh(1)–C(3)	114.6 (9)	P2C11–P(2)–C(dpm)	105.1 (5)
C(1)–Rh(1)–P(1)	90.4 (2)	P2C11–P(2)–Rh(2)	120.2 (3)
H–Rh(1)–C(3)	90 (4)	P2C21–P(2)–C(dpm)	104.7 (4)
H–Rh(1)–P(1)	84.6 (8)	P2C21–P(2)–Rh(2)	109.5 (3)
C(3)–Rh(1)–P(1)	101.1 (1)	C(dpm)–P(2)–Rh(2)	111.5 (4)
P(1)–Rh(1)–P(1)′	155.2 (2)	P(1)–C(dpm)–P(2)	108.5 (6)
C(2)–Rh(2)–H	151 (3)	O(1)–C(1)–Rh(1)	180 (2)
C(2)–Rh(2)–C(3)	112.3 (8)	O(2)–C(2)–Rh(2)	177 (2)
C(2)–Rh(2)–P(2)	90.4 (2)	O(3)–C(3)–Rh(1)	138 (1)
H–Rh(2)–C(3)	97 (3)	O(3)–C(3)–Rh(2)	142 (2)
H–Rh(2)–P(2)	82.5 (7)	Rh(1)–C(3)–Rh(2)	79.4 (7)
C(3)–Rh(2)–P(2)	103.75 (9)	Rh(1)–H–Rh(2)	94 (5)
P(2)–Rh(2)–P(2)′	149.9 (2)	O(PTS1)–S–O(PTS2)	113.3 (6)
P1C21–P(1)–P1C11	104.8 (4)	O(PTS1)–S–O(PTS1)′	113 (1)
P1C21–P(1)–C(dpm)	105.2 (4)	O(PTS2)–S–S1C11	107.2 (8)
P1C21–P(1)–Rh(1)	120.5 (3)	O(PTS1)–S–S1C11	104.8 (6)
P1C11–P(1)–C(dpm)	104.1 (4)	C(PTS)–S–S1C13	117 (1)
P1C11–P(1)–Rh(1)	110.1 (3)	C(PTS)–S–S1C15	123 (2)
C(dpm)–P(1)–Rh(1)	110.8 (4)		

(34) (a) Mills, O. S.; Nice, J. P. *J. Organomet. Chem.* **1967**, *10*, 337. (b) Mills, O. S.; Paulus, E. F. *Ibid.* **1967**, *10*, 331.
(35) Albano, V. S.; Sansoni, M.; Chini, P.; Martinego, S.; Strumolo, D. *J. Chem. Soc., Dalton Trans.* **1976**, 970.
(36) Ciani, G.; Garlaschelli, L.; Manassero, M.; Sartorelli, U. *J. Organomet. Chem.* **1977**, *129*, C25.
(37) Corey, E. R.; Dahl, L. F.; Beck, W. *J. Am. Chem. Soc.* **1963**, *85*, 1202.
(38) Wei, C. H. *Inorg. Chem.* **1969**, *8*, 2385.
(39) (a) Bau, R.; Teller, R. G.; Kirtley, S. W.; Koetzle, T. F. *Acc. Chem. Res.* **1979**, *12*, 176. (b) Churchill, M. R.; Lashewycz, R. A. *Inorg. Chem.* **1979**, *18*, 3261.
(40) Hoffmann, R., personal communication. Hoffman, D. M.; Hoffmann, R. *Inorg. Chem.* **1981**, *20*, 3543–3555.

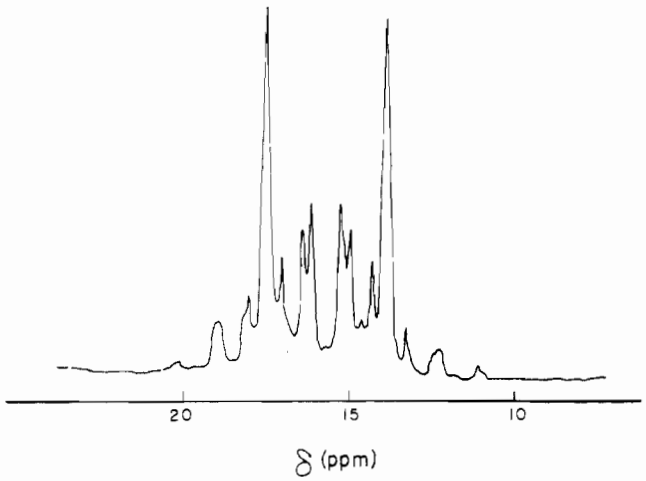

Figure 4. $^{31}P\{^1H\}$ NMR spectrum of $[Rh_2(\mu\text{-}CO)(CO)_2(dpm)_2]$. Chemical shifts in ppm downfield of internal trimethyl phosphate.

Å, correspond to reported values.[3,5,41] The S–O, S–C, and CH_3–C distances of 1.44 (1), 1.75 (1), and 1.58 (4) Å, respectively, are in complete agreement with other structurally characterized *p*-toluenesulfonates.[42]

The two THF molecules are thermally disordered and show chemically unreasonable average C–C bond lengths of 1.29 (6) Å. An indication of the degree of thermal disorder is that while the two THF molecules show the stable five-membered ring conformations of C_s "envelope" and C_2 "half-chair",[43] they are much less pronounced than the idealized conformations. The disorder appears to have the effect of averaging the THF carbon and oxygen atomic positions to values which correspond to severely flattened THF molecules with unrealistic bond lengths. The displacements of the oxygen and carbon atoms from the least-squares plane through the THF molecule with C_s symmetry are for O, 0.06, for Cl, –0.05, and for C(2), 0.02, which are to be compared with the ideal values for O, 0.63, for Cl, –0.51, and for C(2), 0.20 Å.[43] The actual vs. idealized values for the THF molecules with C_2 symmetry are for O, 0.0, for Cl, –0.06, and for C(2), 0.13, which should be compared to values for O, 0.0, for Cl, –0.37, and for C(2), 0.60.

There are no unusual intra- or intermolecular contacts in the structure. The solvent THF molecules, *p*-toluenesulfonate, and $[Rh_2(\mu\text{-}H)(\mu\text{-}CO)(CO)_2(dpm)_2]^+$ cation are all well separated from each other. The closest approaches of the anion and cation involve the *p*-toluenesulfonate oxygen atoms and dpm phenyl H atoms: O(PTS1)···P1H12 = 2.36 (1), O(PTS1)···P2H22 = 2.41 (2) Å. All phenyl H···H distances in the structure are greater than the sum of van der Waals radii (2.4 Å). The closest inter- and intramolecular phenyl H···H distances are P1H13···P1H14 = 2.56 (2) and P2H25···P2H26 = 2.52 (2) Å, respectively.

Additions of Acetylenes. The unsaturated Rh(0) complex $[Rh_2(CO)_2(dpm)_2]$ adds other substrates besides CO and H^+. Acetylene reacts to produce intense emerald green solutions which contain $[Rh_2(C_2H_2)(CO)_2(dpm)_2]$. The acetylene adduct exhibits two ν(CO) at 1946 s,sh and 1938 vs cm^{-1} (benzene solution). The acetylenic proton resonances were not observed in the ^1H NMR spectrum and possibly overlap other resonances. The $^{31}P\{^1H\}$ NMR spectrum shows a symmetric multiplet centered at δ 17.66 with two principal lines separated by 133 Hz and features extremely similar to the spectrum of $[Rh_2(\mu\text{-}CO)(CO)_2(dpm)_2]$ (Figure 4). The corresponding blue-green phenylacetylene complex $[Rh_2(PhCCH)(CO)_2(dpm)_2]$ is prepared by the addition of 1 equiv of phenylacetylene to a solution of $[Rh_2(CO)_2(dpm)_2]$. The phenylacetylene adduct is characterized by ν(CO), at 1958 vs, 1930 s, sh cm^{-1}, and a very complex $^{31}P\{^1H\}$ NMR spectrum with none of the symmetry seen for the normal acetylene adduct. Attempts to prepare a diphenylacetylene complex have been unsuccessful, presumably a consequence of incompatible steric requirements of the dpm and diphenylacetylene phenyl rings.

Balch has reported the additions of activated acetylenes, hexafluoro-2-butyne and dimethyl acetylenedicarboxylate, to $[Pd_2Cl_2(dpm)_2]$,[12a] and more recently, Cowie has described the addition of these same acetylenes to $[RhCl(CO)(dpm)]_2$ and $[Rh_2(\mu\text{-}CO)Cl_2(dpm)_2]$.[12b] The adducts $[Pd_2(\mu\text{-}CF_3C{\equiv}CCF_3)Cl_2(dpm)_2]$ and $[Rh_2(\mu\text{-}CH_3CO_2C{\equiv}CCO_2CH_3)(\mu\text{-}CO)Cl_2(dpm)_2]$ were found by X-ray studies to possess the structural arrangement of dimetalated olefins. The available spectroscopic data are insufficient to determine the mode of acetylene bonding in the present Rh(0) complexes.

The acetylene complex $[Rh_2(HCCH)(CO)_2(dpm)_2]$ reacts with H_2 when solutions of it are heated. Under an atmosphere of 2:1 H_2/C_2H_2, toluene solutions of $[Rh_2(CO)_2(dpm)_2]$ at 80 °C hydrogenate acetylene to ethane at a rate of ca. 3.3 mol of ethane (mol of complex)$^{-1}$ h^{-1}. No cyclotrimerization is observed, and the rate of acetylene reduction to ethane is greater than the rate of ethylene hydrogenation under similar conditions (ca. 0.1 turnover/h). Recently, Sanger has demonstrated the effectiveness of the cationic A-frame complex $[Rh_2(\mu\text{-}Cl)(CO)_2(dpm)_2]^+$ for the hydrogenation of alkynes and alkenes.[7b]

Addition of CO_2 and the Preparation and Reactions of $[Rh_2(\mu\text{-}O_2CH)(CO)_2(dpm)_2]$. The addition of CO_2 to $[Rh_2(CO)_2(dpm)_2]$ is accomplished in dry THF solutions at low temperature and leads to $[Rh_2(CO_2)(CO)_2(dpm)_2]$ as a pale yellow precipitate. The complex displays ν(CO) at 1954 s and 1941 vs and additional peaks attributed to $\nu(CO_2)$ at 1645 m and 1590 s cm^{-1} (Nujol). These values compare favorably with values of 1660 and 1635 cm^{-1} reported by Aresta and Nobile[43] for $Ni(CO_2)(PR_3)_2$ complexes. Further characterization by spectroscopic methods requiring solution samples has been frustrated by the facile dissociation of CO_2 with reversion to $[Rh_2(CO)_2(dpm)_2]$.

The reaction chemistry which has been attempted is found to lead only to the products which would be expected from similar reactions with $[Rh_2(CO)_2(dpm)_2]$ alone. Thus, the addition of 1 equiv of CO produces the Rh(0) carbonyl A-frame complex $[Rh_2(\mu\text{-}CO)(CO)_2(dpm)_2]$ as well as 1 equiv of CO_2. The protonation of the CO_2 complex leads to $[Rh_2(H)(CO)_2(dpm)_2]^+$ and CO_2.

Although direct protonation of the CO_2 complex causes CO_2 loss, a μ-formato complex, $[Rh_2(\mu\text{-}O_2CH)(CO)_2(dpm)_2]^+$, can be prepared by heating the hydride species $[Rh_2(H)(CO)_2(dpm)_2]^+$ in the presence of excess CO_2 for ca. 5 min. The red formate complex is obtained analytically pure and exhibits ν(CO) of 1946 vs, and 1968 vs and an additional stretch at 1548 cm^{-1} (Nujol) in the region characteristic of η^2 or bridging carboxylate ligands.[44-51] The formate complex can also be

(41) Vidal, J. L.; Fiato, R. A.; Pruett, R. L. *Inorg. Chem.* **1978**, *17*, 2574.
(42) (a) Couldwell, C.; Prout, K.; Robey, D.; Taylor, R.; Rossotti, F. J. C. *Acta Crystallogr., Sect. B* **1978**, *34*, 1491. (b) Eliel, E. L. "Stereochemistry of Carbon Compounds"; McGraw-Hill: New York, 1962; p 250.
(43) Aresta, M.; Nobile, C. F. *J. Chem. Soc., Dalton Trans.* **1977**, 708.
(44) Johnson, S. A.; Hunt, H. R.; Neumann, H. M. *Inorg. Chem.* **1963**, *2*, 960.
(45) Vol'pin, M. E.; Kolomnikov, I. S. *Organomet. React.* **1975**, *5*, 313.
(46) Eisenberg, R.; Hendriksen, D. E. *Adv. Catal.* **1979**, *28*, 79.
(47) Immirzi, A.; Musco, A. *Inorg. Chim. Acta* **1977**, *24*, L49.
(48) Yoshida, T.; Thorn, D. L.; Okano, T.; Ibers, J. A.; Otsuka, S. *J. Am. Chem. Soc.* **1979**, *101*, 4212.
(49) Yoshida, T.; Ueda, Y.; Otsuka, S. *J. Am. Chem. Soc.* **1978**, *100*, 3941.
(50) Balch, A. L.; Tulyathan, B. *Inorg. Chem.* **1977**, *16*, 2840.
(51) Smith, S. A.; Blake, D. M.; Kubota, M. *Inorg. Chem.* **1972**, *11*, 660.

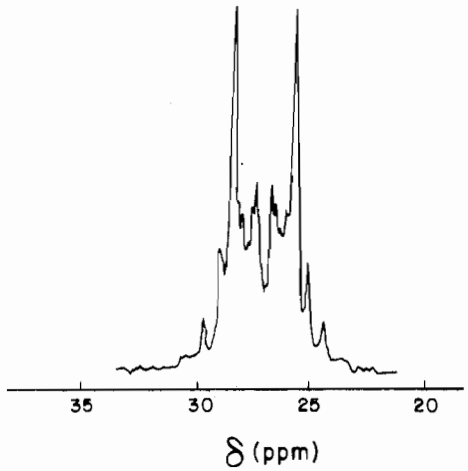

Figure 5. $^{31}P\{^1H\}$ NMR spectrum of $[Rh_2(\mu\text{-}H)(\mu\text{-}CO)(CO)_2(dpm)_2]^+PF_6^-$. Chemical shifts in ppm downfield of internal trimethyl phosphate.

prepared independently from $[Rh_2Cl_2(CO)_2(dpm)_2]$ and $NaHCO_2$. The insertion of CO_2 into M–H bonds has a number of precedents in the chemistry of mononuclear hydride complexes.[45-49] The two methods of preparation and proposed structure, III, of the formate complex are summarized in eq 4. We have also prepared the corresponding acetate complex

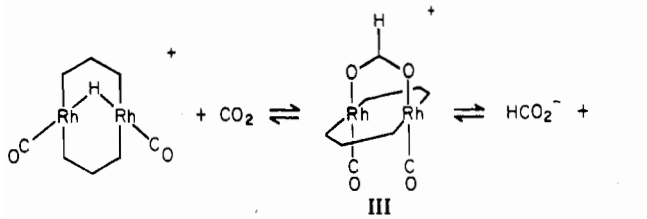

$[Rh_2Cl_2(CO)_2(dpm)_2]$ (4)

from $NaCH_3CO_2$; it too is red and shows ν(CO) at 1951 vs and 1974 vs and $\nu(CH_3CO_2)$ at 1520 cm^{-1} (Nujol). A related neutral diacetate complex, $[Rh_2(\mu\text{-}O_2CCH_3)_2(CO)_2(dpm)_2]$, has been reported by Balch and has similar color and IR data as the present μ-carboxylate complexes.[50]

An unusual reaction of the formate complex $[Rh_2(\mu\text{-}O_2CH)(CO)_2(dpm)_2]^+$ is its rapid decomposition in the presence of CO. The products of the reaction are CO_2 and $[Rh_2(\mu\text{-}H)(\mu\text{-}CO)(CO)_2(dpm)_2]^+$ according to eq 5. In

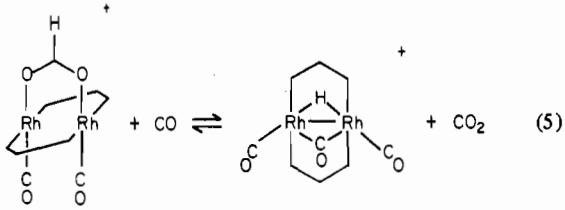

(5)

contrast, the closely related acetate complex does not show any evidence of reaction with CO. The decomposition of formate to hydride and CO_2 may proceed via a change in formate coordination from bridging to terminal followed by decarboxylation through a β-elimination step

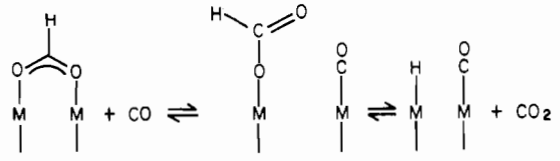

Kubota has reported reactions of Ir η^2-carboxylates with CO which produce the corresponding η^1-carboxylate, carbonyl complexes.[51] Masters has recently reported an apparently similar "β-elimination" of hydride from a η^1-formate complex of iridium to give CO_2 and the corresponding iridium hydride.[52]

Scheme II

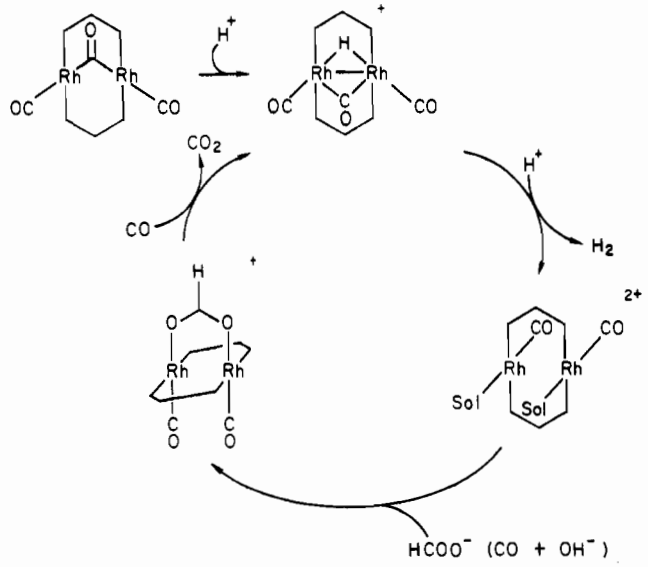

Water-Gas Shift Catalysis. Two independent observations regarding the reaction chemistry of $[Rh_2(\mu\text{-}H)(\mu\text{-}CO)(CO)_2(dpm)_2]^+$ suggest the possibility of water-gas shift (WGS) catalysis (eq 6). The first is decomposition of the

$$H_2O + CO \rightleftharpoons CO_2 + H_2 \qquad (6)$$

formate complex in the presence of CO to produce the hydride $[Rh_2(\mu\text{-}H)(\mu\text{-}CO)(CO)_2(dpm)_2]^+$ and CO_2 (eq 5). The second observation is that hydrogen can be produced by treating $[Rh_2(\mu\text{-}H)(\mu\text{-}CO)(CO)_2(dpm)_2]^+$ with acid. For example, the reaction of $[Rh_2(\mu\text{-}H)(\mu\text{-}CO)(CO)_2(dpm)_2]^+$ with HCl under CO leads to the immediate production of 1 equiv of H_2 and the μ-Cl, μ-CO complex $[Rh_2(\mu\text{-}Cl)(\mu\text{-}CO)(CO)_2(dpm)_2]^+$, first reported by Sanger et al.[3] A similar reaction with $HClO_4$ yields H_2 and the solvated dication $[Rh_2(CO)_2(Sol)_2(dpm)_2]^{2+}$, which can be formed independently from $Rh_2Cl_2(CO)_2(dpm)_2$ and $AgBF_4$. These observations together with the established preparation of the formate complex form $[Rh_2Cl_2(CO)_2(dpm)_2]$ and HCO_2^- form a complete cycle of steps sufficient for water-gas shift catalysis. While this proposal led us to discover the activity of $[Rh_2(\mu\text{-}H)(\mu\text{-}CO)(CO)_2(dpm)_2]^+$ as a WGS catalyst, the reactions shown in Scheme II do not necessarily represent actual steps in the catalysis.

Both method A and method B (see Experimental Section) produced stoichiometric amounts of CO_2 and H_2 while consuming a stoichiometric amount of CO. In a typical run with method A, 0.39 mmol of CO was converted into 0.39 mmol of CO_2 and 0.39 mmol of H_2 in 15 h. Employing method B resulted in the consumption of 0.53 mmol of CO and the production of 0.53 mmol of CO_2 and 0.53 mmol of H_2 in 15 h.

The most active catalytic systems contain $[Rh_2(\mu\text{-}CO)(CO)_2(dpm)_2]$, 1 equiv of *p*-toluenesulfonic acid and 2 equiv of a salt (i.e., LiCl, LiBr, NaCl) in 1-propanol solution. The rates of catalysis at 90 °C for the most active systems using previously established procedures[53] and GC analysis of the

(52) Masters, C. *Adv. Organomet. Chem.* **1979**, *17*, 61.
(53) Cheng, C. H.; Hendriksen, D. E.; Eisenberg, R. *J. Am. Chem. Soc.* **1977**, *99*, 2791.
(54) Laine, R. M.; Rinker, R. G.; Ford, P. C. *J. Am. Chem. Soc.* **1977**, *99*, 252.
(55) Cheng, C. H.; Eisenberg, R. *J. Am. Chem. Soc.* **1978**, *100*, 5968.
(56) Ford, P. C.; Rinker, R. G.; Ungermann, C.; Laine, R. M.; Landis, V.; Moya, S. A. *J. Am. Chem. Soc.* **1978**, *100*, 4595.

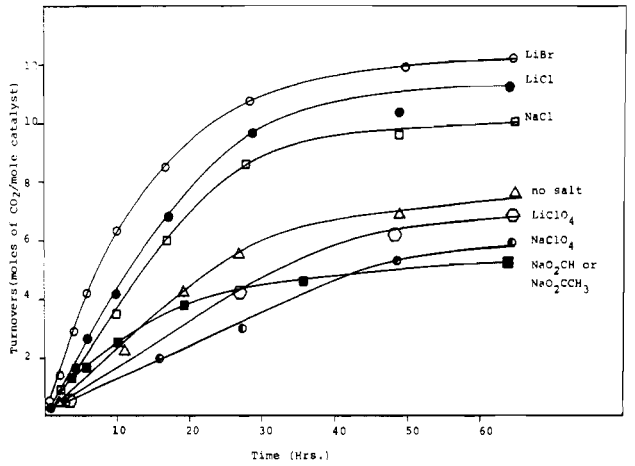

Figure 6. Plot of turnovers vs. time illustrating the effect of various salts on the catalysis of the WGSR.

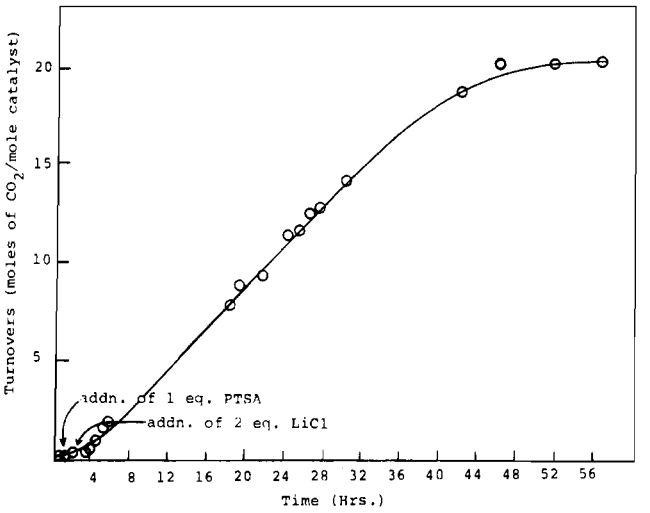

Figure 7. Plot of turnovers vs. time for the hydroformylation/hydrogenation of ethylene.

gases above the catalyst solutions correspond to 0.58 turnover/h. The catalysis continues at this rate for approximately 35 h, after which the rate gradually decreases until cessation of catalysis after 70 h. The highest rates of catalysis are obtained at nearly neutral pH conditions. Excess acid or base results in decomposition of the catalyst complex. The effect of different salts on the catalysis is shown in Figure 6. No simple explanation of the rate differences is apparent. While LiBr, LiCl, and NaCl appear to enhance the catalysis, we also find that the halo-bridged complex $[Rh_2(\mu\text{-}X)(CO)_2(dpm)_2]^+$ (X = Cl, Br), which can form by the reaction of $[Rh_2(CO)_2(Sol)_2(dpm)_2]^{2+}$ with X^-, is inactive as a catalyst precursor when used in a similar run. Carboxylate salts appear to slow the reaction. Surprisingly, this observation includes formate which we initially proposed as the species by which CO + OH^- enter the catalytic cycle shown in Scheme II. We do not have direct evidence for formate involvement in the catalysis and note that other species such as hydroxycarbonyls may actually be involved. In any case the effect of added salts is not a major one and may simply relate to a medium effect. Finally, the deactivation of the catalyst is observed in all systems tried. Further studies designed to uncover the nature of the deactivated catalyst and to maintain the lifetime of the active catalyst are in progress.

Hydroformylation/Hydrogenation Catalysis. The same conditions employed in the WGS catalysis system also catalyze the hydroformylation of ethylene to propanal via the Reppe modification, as well as the hydrogenation by CO + H_2O, of both ethylene to ethane and propanal to 1-propanol. The rate of hydroformylation catalysis based on CO_2 production is 0.52 turnovers/h for approximately 35 h. Analysis of the reduction products at the end of catalysis indicates the formation of approximately 25% propanal, 25% hydrogen, 15% ethane, and 5% 1-propanol compared with CO_2 which is the only oxidation product formed (each reduction step requires the formation of 1 molecule of CO_2). A typical run is shown in Figure 7. The strong dependence of the activity of this system on the presence of a salt (e.g., LiCl) is also indicated during the first few hours of the run.

If, in addition to CO and ethylene, H_2 is present, the catalyst system promotes hydrogenation more effectively than hydroformylation. The amount of ethane produced is eight times greater than that of propanal. The rate of hydrogenation is also faster than for Reppe hydroformylation, being 7.5 turnovers/h for the ethylene-to-ethane conversion on the basis of GC analysis of ethane produced when commencing with 300-torr CO, 150-torr C_2H_4, and 150-torr H_2 at 90 °C. The catalyst also hydrogenates propanal to 1-propanol in the presence of H_2.

The slowness of hydroformylation via the Reppe modification and the near identity of the rate of this reaction with that of water-gas shift strongly suggest similar slow steps in the two catalyses. The observation of increased amounts of ethane when H_2 is present vs. the product distribution when the Reppe modification of hydroformylation is followed without added H_2 rules against a two-stage hydroformylation process in which H_2 is initially formed via WGS and then consumed via conventional hydroformylation.

These conclusions and the experiments on which they are based are under continuing study.

Conclusions

We have shown that the binuclear Rh(0) complex $[Rh_2(CO)_2(dpm)_2]$ and its apparent solvated isomer $[Rh_2(\mu\text{-}CO)(CO)(dpm)_2(Sol)]$ are capable of adding numerous small molecule substrates. A-Frame complexes result from the addition of CO, H^+, acetylenes, and possibly CO_2. The activity of several of these complexes as homogeneous catalysts is significant. An acetylene A-frame complex $[Rh_2(HCCH)(CO)_2(dpm)_2]$ is found to efficiently reduce acetylene to ethane. An unusual μ-hydride, μ-carbonyl complex is prepared by the addition of H^+ and CO to $[Rh_2(CO)_2(dpm)_2]$. The structure of $[Rh_2(\mu\text{-}H)(\mu\text{-}CO)(CO)_2(dpm)_2]^+(p\text{-}CH_3C_6H_4SO_3)^-\cdot 2THF$ was determined by X-ray crystallography and shows a μ-hydride A-frame skeleton with a carbon monoxide bridging the two Rh centers in the endo pocket. This μ-hydride, μ-carbonyl complex is also prepared by the reaction of a μ-formato complex with CO and shows high activity in the water-gas shift reaction as well as in the catalysis of the hydroformylation of ethylene.

Acknowledgment. We wish to thank the National Science Foundation (Grant No. CHE 80-11974) and the donors of the Petroleum Research Fund, administered by the American Chemical Society, for support of this research. A generous loan of precious metal salts from Johnson Matthey Co., Inc., is also gratefully acknowledged. C.P.K. wishes to acknowledge a Elon Huntington Hooker Fellowship and a Sherman Clarke Fellowship.

Registry No. $[Rh_2(\mu\text{-}4)(\mu\text{-}CO)(CO)_2(dpm)_2]\text{-}p\text{-}CH_3C_6H_4SO_3\cdot 2THF$, 80924-10-3; $Rh_2(CO)_2(dpm)_2$, 74507-89-4; $Rh_2(\mu\text{-}CO)(CO)(dpm)_2(PPh_3)$, 80865-87-8; $Rh_2(\mu\text{-}CO)(CO)_2(dpm)_2$, 74507-92-9; $Rh_2(HCCH)(CO)_2(dpm)_2$, 80846-10-2; $Rh_2(HCCPh)(CO)_2$-

(57) Kang, H. C.; Mauldon, C. H.; Cole, T.; Slegeir, W.; Cann, K.; Pettit, R. *J. Am. Chem. Soc.* **1977**, *99*, 8323.
(58) King, R. B.; Frazier, C. C.; Hanes, R. M.; King, A. D. *J. Am. Chem. Soc.* **1978**, *100*, 2925.
(59) Mague, J. T.; DeVries, S. H. *Inorg. Chem.* **1980**, *19*, 3743.

$(dpm)_2$, 80846-11-3; $Rh_2(CO_2)(CO)_2(dpm)_2$, 80865-88-9; $[Rh_2(H)(CO)_2(dpm)_2]PF_6$, 80846-12-4; $[Rh_2(H)(CO)_2(dpm)_2]$-p-$CH_3C_6H_4SO_3$, 74507-91-8; $[Rh_2(\mu\text{-}O_2CH)(CO)_2(dpm)_2]PF_6$, 80846-14-6; $[Rh_2(\mu\text{-}O_2CCH_3)(CO)_2(dpm)_2]BF_4$, 80846-15-7; $[Rh_2(\mu\text{-}H)(\mu\text{-}CO)(CO)_2(dpm)_2]PF_6$, 80876-88-6; $[Rh_2(\mu\text{-}Cl)(CO)_2(dpm)_2]PF_6$, 80448-77-7; $[Rh_2(\mu\text{-}Cl)(\mu\text{-}CO)(CO)_2(dpm)_2]^+$, 67202-36-2; $Rh_2Cl_2(CO)_2(dpm)_2$, 22427-58-3; $RhH(CO)(PPh_3)_3$, 17185-29-4.

Supplementary Material Available: Listing of observed and calculated structure factors (7 pages). Ordering information is given on any current masthead page.

Contribution from the School of Chemical Sciences, University of Illinois, Urbana, Illinois 61801

Asymmetric Hydrogenation: Chiral Bis(phosphine)rhodium Catalysts with Phenyl Group Derivatives

TADATSUGU YOSHIKUNI and JOHN C. BAILAR, JR.*

Received November 30, 1981

Some attempts to achieve optically active products were carried out by new catalysts of the type $[Rh(COD)(P^*)_2]^+$, where the chiral phosphorus ligands are α-naphthylphenyl(o- or p-tolyl)phosphine (NPTP), bis[phenyl(o- or p-tolyl)phosphino]ethane (BPTE), bis(α-naphthylphenylphosphino)ethane (BNPE), and 1-phenyl-1,2-bis(diphenylphosphino)ethane (R-PDPE). Optical yields of 50–75% ee (ee = enantiomeric excess) were obtained in the hydrogenation of acetamidoacrylic acid. The ortho isomer of the tolyl group gave a higher optical yield than the para one. Isoalcohols were effective solvents. It was found that these catalysts can be recovered and reused for asymmetric hydrogenation.

Introduction

Many studies (for example, ref 1–4) of selective asymmetric hydrogenation with metal catalysts have been made. Ligands which have optical activity on an atom of phosphorus, nitrogen, or carbon can give optically active products. It has been said that ligands containing optically active phosphorus atoms are more effective than others, but in recent years it has been shown that ligands having optical activity on carbon[5] and nitrogen[6] may be very effective for asymmetric hydrogenation. Many asymmetric hydrogenation catalysts are sensitive to air and moisture, so they require special handling.

We have prepared catalysts which are stable in air and effective for asymmetric hydrogenation. The ligands described have optical activity residing on a phosphorus atom (P* or $\overline{P^*P^*}$) and contain phenyl, tolyl, and naphthyl groups. Those compounds were expected to give complexes having large optical activity because of their bulky structures. Also 1-phenyl-1,2-bis(diphenylphosphino)ethane[7] (R-PDPE or R-phenphos) was used as a typical aromatic ligand having optical activity on one carbon atom.

Results and Discussion

Ligand I, NPTP, is monodentate, so it presents the possibility that either one or two groups may coordinate to give $[Rh(COD)(P^*)X]$ or $[Rh(COD)(P^*)_2]X$. The first was tested by using the monophosphine complex for hydrogenation of α-acetamidoacrylic acid. However, so the completely hydrogenated product could be obtained, it was found that the hydrogenation had to be carried out with a relatively large concentration of catalyst (S/Rh = 5). The reaction was slow. On the other hand, the rhodium compound containing two monophosphine molecules was effective under moderate conditions. Therefore, in all later studies on asymmetric hydrogenation, we used bidentate phosphine rhodium compounds.

The ligands described in this paper are shown in Figure 1. Ligands I and II each exist in two isomeric forms (ortho and para), both optically active. The other ligands exist as meso-, levo-, and dextrorotatory isomers. Optical resolutions were carried out by fractional precipitation of the D-α-bromocamphor-π-sulfonate (BCS)–rhodium compounds. In each case, the fractional precipitation was repeated until the limiting optical activity was obtained. The resulting optically active compounds were converted to the desired salts as described in the Experimental Section.

Figure 2 shows the relationship between hydrogenation yield and time of reaction. All of the catalysts have the ability to completely hydrogenate α-acetamidoacrylic acid in 4 h. Therefore, the following asymmetric hydrogenations (except with the monophosphine catalyst and others especially noted) were carried out under the following conditions: 1 atm pressure, room temperature, substrate/Rh = 50–100, solvent 95% EtOH. Yields at less than 4 h show that all of these catalysts can hydrogenate at about the same rate (Figure 2).

Table I gives the optical yields of products hydrogenated asymmetrically by these catalysts. In general, the optical yield seems to depend upon the magnitude of the optical activity of the catalyst. The optical yield with $[Rh(COD)(NPTP)(H_2O)]^+$ as the catalyst is very much lower than with the diphosphine catalysts. On the other hand, catalysts with diphosphine ligands give good optical yields, especially $[Rh(COD)(BNPE)]^+$. The results suggest that tolyl and phenyl groups on the phosphorus atoms in NPTP exist in the same conformation as in BPTE. If the naphthyl groups in NPTP have the same spatial relationship as do those in BNPE, the yield might be close to the value given by $[Rh(COD)(BNPE)]^+$.

Effects of Catalyst Anions. As noted by Knowles,[8] there is little difference in optical yield when the catalysts contain different anions.

Effects of Position Isomers. The position of the methyl group on the tolyl ring is very important in achieving high

(1) D. Lafont, D. Sinou, and G. Descotes, *J. Mol. Catal.*, **10**, 305 (1981); M. Mazzei, W. Marconi, and M. Riocci, *ibid.*, **9**, 381 (1980).
(2) J. M. Townsend and J. F. Blount, *Inorg. Chem.*, **20**, 269 (1981).
(3) W. S. Knowles and M. J. Sabacky, *Chem. Commun.*, 1445 (1968).
(4) Vesna Čaplar, Giovanni Comisso, and Vitomir Šunjić, *Synthesis*, 85 (1981).
(5) M. D. Fryzuk and B. Bosnich, *J. Am. Chem. Soc.*, **100**, 5491 (1978).
(6) M. Fiorini and G. M. Giongo, *J. Mol. Catal.*, **5**, 303 (1979).
(7) R. B. King, J. Bakos, C. D. Hoff, and L. Marko, *J. Org. Chem.*, **44**, 1729 (1979).
(8) B. D. Vineyard, W. S. Knowles, M. J. Sabacky, G. L. Bachman, and D. J. Weinkauff, *J. Am. Chem. Soc.*, **99**, 5946 (1977).

0020-1669/82/1321-2129$01.25/0